FINAL REPORT

Project J5

March 2023

Assessing & Addressing Deficiencies in the HCM Weaving Segment Analyses (Phase II)

Dr. Nagui Rouphail | North Carolina State University/Kittelson & Associates, Inc.
Dr. Lily Elefteriadou |University of Florida
Dr. Ehsan Amini| University of Florida
Dr. Ishtiak Ahmed | North Carolina State University

STRIDE | Southeastern Transportation Research, Innovation, Development and Education Center

UF | Transportation Institute UNIVERSITY of FLORIDA

DISCLAIMER

The contents of this report reflect the views of the authors, who are responsible for the facts and the accuracy of the information presented herein. This document is disseminated in the interest of information exchange. The report is funded, partially or entirely, by a grant from the U.S. Department of Transportation's University Transportation Centers Program. However, the U.S. Government assumes no liability for the contents or use thereof.

ACKNOWLEDGEMENT OF SPONSORSHIP AND STAKEHOLDERS

This work was sponsored by a grant from the Southeastern Transportation Research, Innovation, Development, and Education Center (STRIDE).

Funding Agreement Number - 69A3551747104

LIST OF AUTHORS

Lead PI: *Nagui M Rouphail, Ph.D.*
North Carolina State University and Kittelson & Associates, Inc.
rouphail@ncsu.edu

Co-PI: *Lily Elefteriadou, Ph.D.*
University of Florida Transportation Institute
elefter@ce.ufl.edu

Additional Researchers:

Ehsan Amini, Ph.D.
University of Florida
amini.e@ufl.edu

Ishtiak Ahmed, Ph.D., PE
Institute for Transportation Research and Education, North Carolina State University
iahmed2@ncsu.edu

TABLE OF CONTENTS

LIST OF FIGURES

LIST OF TABLES

ABSTRACT

In an earlier study (Phase I of the project) the research team developed a new speed and capacity estimation method for ramp weaves. In this phase of the study, the team extends that work to major weaves, develops a speed model for all weaving types, and proposes an alternate capacity estimation process. Two lane-configuration parameters were introduced in the speed model the team developed earlier, in order to make it applicable to all types of weaves. The model was calibrated separately for ramp and major weaves. The resultant root-mean-squared error (RMSE) was 3.46 and 2.36 mi/h, respectively, for major and ramp weaves. The application of the models to the corresponding test/ validation dataset not used in the model development also yielded satisfactory RMSE values—4.7 mi/h for major and 2.56 mi/h for ramp weaves. The team proposed a new capacity model which eliminated the limitation of the previous capacity model for low-volume conditions. However, the difference in the capacity estimates from these two approaches diminishes as the observed flow rate approaches capacity. Both approaches showed remarkably higher sensitivity to segment length than the HCM model, whereas the HCM model exhibited a slightly higher sensitivity to weaving ratio. Overall, the proposed models demonstrated consistency across all types of weaves and with the fundamental speed–flow–capacity relationship. They require fewer inputs than the HCM models, have fewer sub-models, use inputs that are more likely to be available to practitioners, and are sensitive to most of the inputs included in the model.

Keywords: Weave, Traffic speed, Capacity, Highway Capacity Manual, Lane configuration.

EXECUTIVE SUMMARY

In recent years, practitioners have found several cases where the latest Highway Capacity Manual (HCM6 and HCM7) method described in Chapters 13 and 27 cannot model or show sensitivity to certain important weaving segment parameters under certain operating conditions. In an earlier study, the research team developed a new speed and capacity estimation method for ramp weaves. In this study, the team extends that work to major weaves, develops a speed model for all weaving types, and proposes an alternate capacity estimation process.

As part of the earlier study, the research team had already collected demand volumes and geometry data for 14 major or Type B weaving sites. This dataset is supplemented by a limited set of Type C weave data that the team collected from six sites using drone and ground cameras. The field data suggest a significantly lower density at capacity value than what has been previously assumed at weaving segments (43 pc/mi/ln). Based on this observation, the team used 35 pc/mi/ln as the density at capacity for all types of weaves.

To make the speed model applicable to all types of weaves, two lane-configuration parameters were introduced in the speed model the team developed earlier. The model was re-calibrated separately for ramp and major weaves. The resultant root-mean-squared error (RMSE) was 3.46 and 2.36 mi/h, respectively, for major and ramp weaves. The application of the models to the corresponding test/ validation dataset not used in the model development also yielded satisfactory RMSE values—4.7 mi/h for major and 2.56 mi/h for ramp weaves. However, both models overestimated field speeds for a cluster of low-speed observations, which could be related to some unique traffic operational characteristics (e.g., incidents or weather-induced flow disruptions).

A new capacity model was proposed which eliminated the limitation of the previous capacity model for low-volume conditions. The difference in the capacity estimates from these two approaches is meaningful only when the observed flow rate is low; it diminishes significantly as the observed flow rate approaches capacity. The team tested the sensitivity of these two proposed capacity models and the HCM7 model to segment length, number of lanes, and weaving ratio. The HCM7 model showed minimal sensitivity to segment length, whereas the two proposed models were remarkably sensitive, particularly when the segment length was below 1,000 ft. However, the HCM7 model showed a slightly higher sensitivity to weaving ratio than the proposed models. Application of the models to an example problem revealed that the HCM7 model generates a very low volume-to-capacity (v/c) ratio (0.7) for a speed drop of 12 mi/h, whereas the proposed models yielded a much more sensible v/C of 0.8 associated with the same speed drop. The proposed models have consistency across all types of weaves and with the fundamental speed–flow–capacity relationship. They require fewer inputs than the HCM models, use inputs that are more likely to be available to practitioners, and are sensitive to most of the inputs included in the model. Therefore, the outcomes of this research are expected to be valuable resources for practitioners and researchers.

1. INTRODUCTION

1.1. Background and Motivation

Weaving segments are often critical components of freeway facilities, as they can act as bottlenecks (Ahmed et al., 2018). Any biases or errors that are found within this procedure can significantly effect other types of analyses (e.g., facility-wide and reliability analyses), and in the process significantly brings question into the validity of the entire freeway facility methodology.

Researchers at NC State University and the University of Florida have developed an alternative, simplified approach for estimating capacity and quality of service for ramp weaves in the first phase of this project. This research was motivated by the fact that in recent years, practitioners have found several cases where the latest Highway Capacity Manual (HCM7, 2022) method described in its Chapters 13 and 27 is not able to model or show sensitivity to certain important weaving segment parameters under certain operating conditions. For example, the non-weaving vehicles' speeds in the HCM method are not sensitive to the weaving segment short length (which is the distance between two gore points in the weave segment). In addition, the non-weaving speed is not sensitive to all lane changes within the segment. Finally, the weaving segment capacity model is disconnected from the speed model, which violates the fundamental relationship between speed, density, and flow at capacity. These and other deficiencies have led to questioning the validity of the HCM's weave segment analysis. Furthermore, these deficiencies have gradually led to wide-spreading concerns with facility-wide or travel time reliability analyses that, by default, incorporate weaving segment analyses in their procedures.

This report covers Phase II of Project K2, titled *Assessing and Addressing Deficiencies in the HCM Weaving* Segment *Analyses*. Phase I of this project was limited to the analysis of simple, ramp (or Type A) weaves. Two journal papers summarizing the findings from that phase have already been published by Xu et al. (D. Xu et al., 2020) and Amini et al.(Amini et al., 2021). Phase I included new data collection at 15 sites in the Southeast and Western US, and a new speed predictive model that avoids much of the complexities in the HCM7 method. The Phase I model was found to yield more accurate speed predictions than the current HCM7 methodology. When compared to field speeds, it yielded a much lower Root Mean Square Error or RMSE of 3.98 mph, compared to an RMSE of 9.18 mph for the HCM7 model.

This report documents the extension of the work to major or complex weaves, or Type B and Type C weaving segments, depending on the lane configuration at the weave. Those sites are found at both service and system interchanges. As part of the original Phase I data collection, the research team had already collected demand volumes and geometry data for 14 Type B sites. Those data were not used for model development in that phase. In addition, the team had access to the original 12 sites database developed under project NCHRP 03-75, *Analysis of Freeway*

Weaving Sections which included another 10 Type B weaves (R P Roess et al., 2008). As a result, there was no need for new data collection for this weaving configuration in Phase II. The team did collect a limited set of new volume and configuration data in North Carolina (at six sites) for Type C weaving configuration using drone videos supplemented with ground cameras. This enabled the team to analyze all weaving configurations and facilitated the development of new HCM material that is comprehensive across of most (but not necessarily all) weaving types.

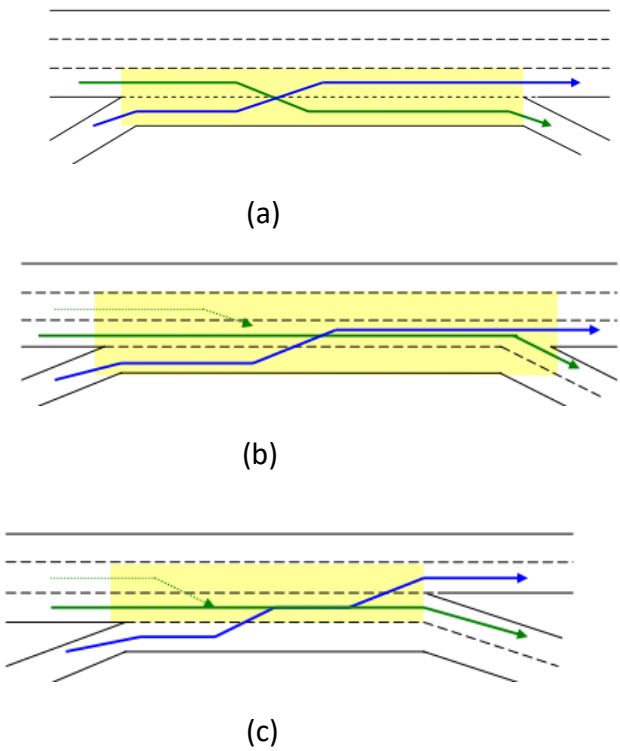

Figure 1-1: Illustration of three common weaving segment types (a) Ramp or Type A weave, (b) Major or complex Type B weave, and (c) Major or Complex Type C weave

Source: NCHRP 03-75 Final Report (2007)

Figure 1-1 depicts the three weaving types covered in this study. The solid lines show the two different weaving maneuvers and the number of lanes required to complete the weave.

1.2. Phase II Scope and Objectives

While the primary objective of this phase is to extend the development of speed and capacity models to major or complex weaves, and therefore close the coverage gap to all weaving segment types, other objectives have emerged since the completion of Phase I that have slightly increased the scope beyond that extension. These include:

- Incorporating weaving segment configuration for *all* segment types. Since Phase I only focused on Type A weaves, a single configuration was covered therefore omitting the need to incorporate any configuration parameters. This incorporation of weave-configuration parameters also applies to work completed in Phase I.
- Improving the estimates of weaving demand volumes for data gathered from mainline and ramp sensors. These sensors are unable to report weaving volumes. A proportional approach was developed and applied to all Type A and B sensor data used in Phases I and II. Type C field data collected with drones was able to directly generate weaving flows.
- Recalibrating Type A speed models to account for both segment configuration parameters and improved estimates of weaving flow rates.
- Coordinate Model Development with NCHRP 07-26*, Update of Highway Capacity Manual: Merge, Diverge, and Weaving Methodologies* (Schroeder, 2019). This parallel national project has adopted the STRIDE project framework developed in Phase I and is applying it beyond weaving segments to include on-ramp and off-ramp junctions. Close coordination is important to facilitate the inclusion of the methods into a future release of the HCM.
- Re-assess the determination of weaving segments' capacity in light of findings from both Phase II and NCHRP 07-26 data.
- Testing the feasibility of using universal speed and capacity models that are applicable to all weaving segment types.

There remains one weaving segment type for which data is lacking. Two-sided weaves are hard to come by and difficult to calibrate. NCHRP 03-75 had a single site, and NCHRP 07-26 had no two-sided weaves in its database. In the interim, the methods used for Type A weaves were adopted for two-sided weaves as well, with the understanding that the weaving flows in this case are the ramp-to-ramp flows. This method is approximate and should be used with caution.

1.3. REPORT ORGANIZATION

This report is organized as follows. Following this introductory chapter, Chapter 2 presents a review of the past studies on weaving segment operations. Chapter 3 documents the field data collection sites and explains the data collection, extraction, and cleaning methodology. Chapter 4 presents the development of the speed and capacity models. Chapter 5 shows the model development and testing results. Finally, Chapter 7 provides conclusions and recommendations for future work in this area.

2. LITERATURE REVIEW

This chapter presents a review of the published literature on weaving segment analysis models. The review includes models that have been adopted in various editions of the HCM and other macroscopic and microscopic models developed.

2.1 History of Weaving Operational Analysis in the HCM

The HCM was first introduced in 1950 (HCM, 1950). Until now, there have been seven major versions of the HCM (in addition to minor revised editions) published. The HCM1950 analyzed weaving segments using six sites and data collected from the Pentagon Network and the San Francisco Bay Bridge. The method considered weaving vehicle behavior and the impact of speed on segment capacity. The relationships between traffic volumes and speed from the six sites are presented in Figure 2-1.

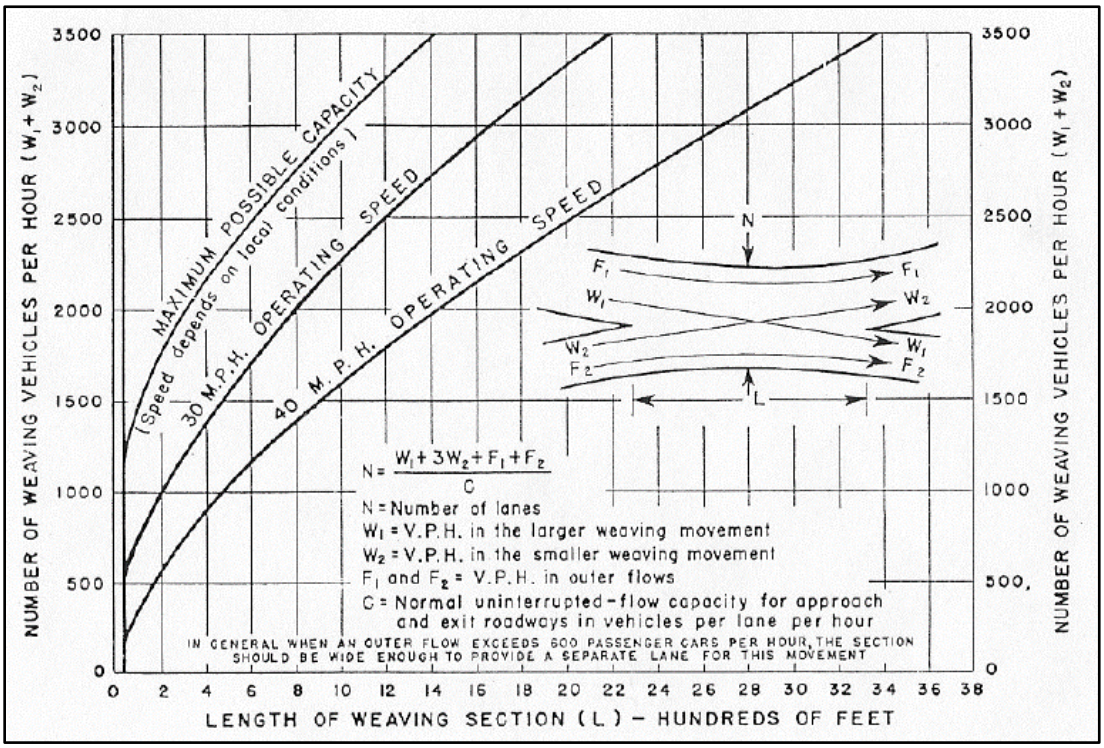

Figure 2-1: HCM1950 traffic volumes and speed relationship plot

In 1965, Leisch and Normann developed a method based on the analysis results of the HCM1950 (Normann, 1957) and their method was added in f types could be further subdivided into one-sided or two-sided sections. The traffic flows in the weaving segment were distinguished as weaving movements and non-weaving movements. The method defined and used the weaving segment length. However, the most important concept in HCM1965 was the development of basic procedures and methodologies to design and evaluate weaving segments. The quality of flow was introduced as a measure of the weaving section operation. As Figure 2-2 shows, the quality of flow had five designated classes (I to V), which represent the congestion level from

light to heavy. Each curve in the figure contained a number known as the k-factor. As stated in the HCM 1965: "The k-factor, in effect, is an equivalency factor expanding the influence of the smaller flow up to a maximum of three times its actual size in number of vehicles." The steps for measuring the weaving section performance were as follows: First, the user locates a point based on segment length and weaving demand. Then, by finding the nearest curve to the point, the class of the quality of flow and the estimated speed can be identified. From Table 7.3 of the HCM1965, which is shown in Table 2-1, the known quality of flow can be converted to the LOS. The capacity of the segment is determined using Table 2.2 (Table 7.2 of HCM1965). However, the capacity was not used in determining the LOS. Even though the HCM1965 included a method for evaluating the segment performance, it was mostly focused on the design of the segment.

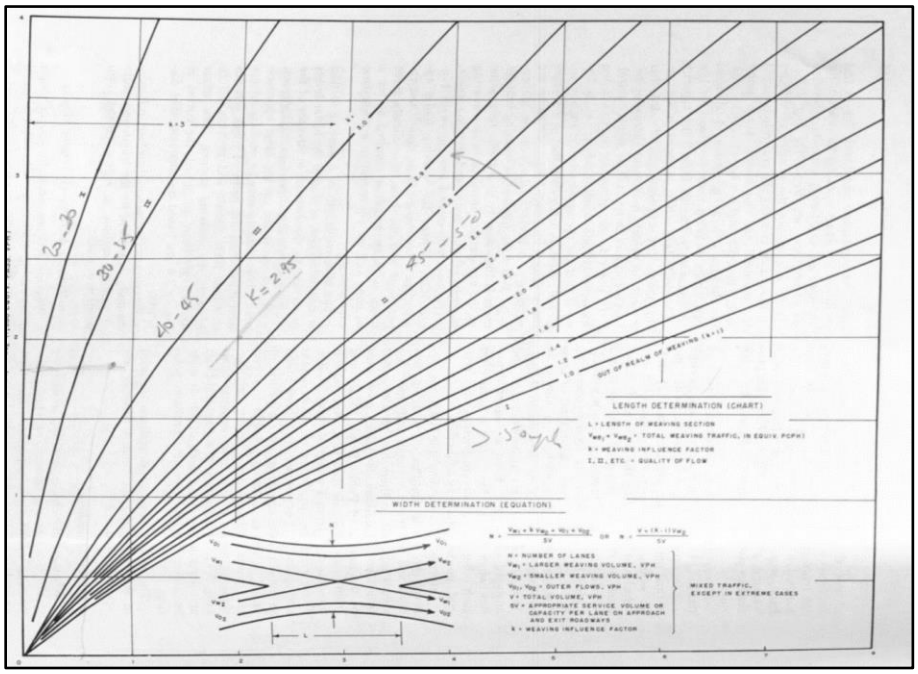

Figure 2-2: Quality of flow curves and relative estimated speeds (HCM1965)

Table 2-1: HCM1965 relationship between LOS and quality of flow on a weaving section

	Quality of Flow			
	Freeways and Multilane Rural Highways			
Level of Service	**Highway Proper**	**Connecting Collector-Distributor Roads and Other Interchange Roadways**	**Two-Lane Rural Highways**	**Urban and Suburban Arterials**
A	I–II	II–III	II	III–IV
B	II	III	II–III	III–IV
C	II–III	III–IV	III	IV
D	III–IV	IV	IV	IV
E	IV–V	V	V	V
F	Unsatisfactory			

Table 2-2: Quality of flow and maximum lane service volumes in a weaving section (HCM1965)

Quality of Flow Curve	Max Lane SV Value (pc/h)
I	2,000
II	1,900
III	1,800
IV	1,700
V	1,600

From 1965 to 1985, several weaving analysis models were developed. Roess and McShane's model appeared in several forms, and its final form was introduced in Circular 212 (Roger P Roess et al., 1980). The model was iterative and intended to predict the average speed of weaving and non-weaving vehicles. In 1984, Reilly developed a model that utilized a density concept tied to weaving intensity to predict the average speed for weaving and non-weaving traffic (Reilly, 1984). The HCM1985 merged these two models (HCM, 1985). Reilly et al.'s model was stratified to different configurations and types of operations. The following equation was used in the HCM1985 to estimate speeds:

$$S_i = 15 + \frac{50}{1 + a(1 + VR^b)\left(\frac{v}{N}\right)^c / L^d}, \tag{2-1}$$

where,

S_i is the average speed (mi/h) in the weaving section i
VR is the volume ratio
v is the total traffic volume (v/hr)
N is the number of lanes
L is the length (ft) of the weaving section
$a, b, c,$ and d are model's parameters.

The equation implies that the traffic speed is related to the volume ratio, traffic demand, number of lanes, and the length of the segment. The four constant parameters (*a*, *b*, *c*, and *d*) in the equation were calibrated considering the type of the segment and type of operation. First, the speed was predicted by using unconstrained operation parameters. Then, by comparing two variables, the number of lanes required for the weaving segment, N_w, and the maximum number of weaving lanes, N_w(max), the assumption for the predicted speed under the unconstrained condition was justified.

The HCM1985 distinguishes between 3 types of weaves (Figure 2-3). For Type A weaving sections, weaving vehicles in each direction must make one lane change, while in Type B sections one of the weaving movements can reach its destination without making any lane changing and the other requires one lane change. In Type C weaving sections, one of the weaving movements can reach its destination without any lane changes, while the other movement requires at least two lane changes.

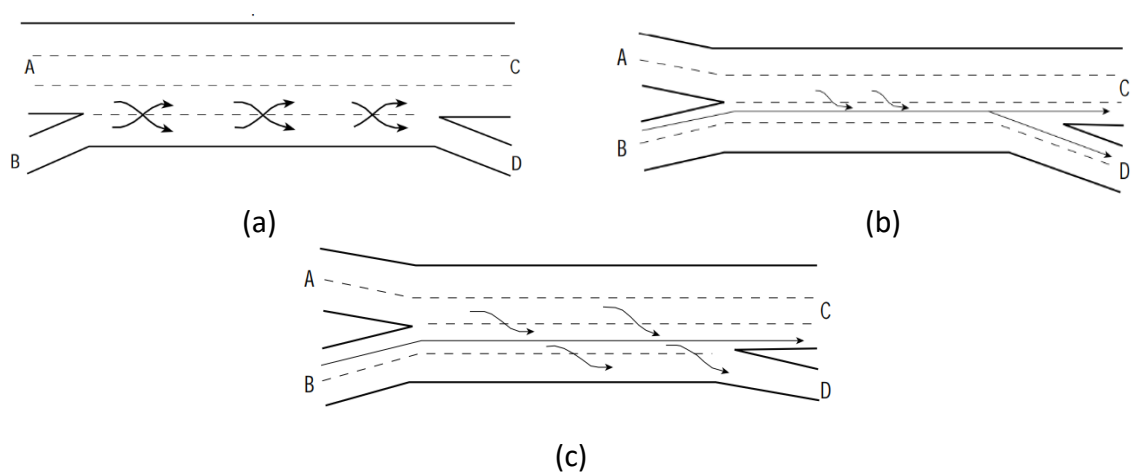

Figure 2-3: Schematic of weaving section a) type A b) type B c) type C

Table **2-3** shows the equations for calculating N_w and N_w(max) for different types of configurations. The speed was predicted using the parameters of the constrained operation if it was shown that traffic was constrained. The predicted speed was then used in the determination of LOS for weaving and non-weaving traffic. Table 2-4 shows the LOS criteria in the HCM1985. The segment's final LOS was the worse LOS between the two.

Table 2-3: Criteria for unconstrained vs. constrained operation of weaving areas (Transportation Research Board, 1985)

Type of Configuration	No. of Lanes Required for Unconstrained Operation, N_W	Max. No. of Weaving Lanes, N_W(max)
Type A	$2.19\ N\ VR^{0.571}\ {L_H}^{0.234}/{S_W}^{0.438}$	1.4
Type B	$N\{0.085 + 0.703\ VR + \left(\frac{234.8}{L}\right) - 0.018\ (S_{NW} - S_W)\}$	3.5
Type C	$N\{0.761 - 0.011\ L_H - 0.005(S_{NW} - S_W) + 0.047\ VR\}$	3.0

Table 2-4: LOS criteria for freeway weaving sections in HCM1985 (Transportation Research Board, 1985)

Level of Service	Minimum Average Weaving Speed, S_W (mph)	Minimum Average Non-Weaving Speed, S_{NW} (mph)
A	55	60
B	50	54
C	45	48
D	40	42
E	35	35
F	<35	<35

The HCM1985 also provided a table of limitations for the analysis of weaving segments, shown in **Table 2-5**. The table includes various limitations or maximum values for input parameters to indicate the conditions under which the LOS predictions were valid.

Table 2-5: HCM1985 Limitations on weaving analysis (Transportation Research Board, 1985)**.**

Type of Configuration	Weaving Capacity Maximum, v_w	Maximum, *v/N* *(pc/h/ln)*	Maximum Volume Ratio, *VR*	Maximum Weaving Ratio, *R*	Maximum Weaving Length, *L*
Type A	1,800 pc/h	1,900	*N* *VR* 2 1.00 3 0.45 4 0.35 5 0.22	0.5	2,000 ft
Type B	3,000 pc/h	1,900	0.80	0.5	2,500 ft
Type C	3,000 pc/h	1,900	0.50	0.4	2,500 ft

The HCM1985 method was revised several times, but the model form was still used in HCM2000. In 1998, the HCM revised the table of limitations and the LOS criteria (HCM, 2000). The HCM1997 used the average density of all the vehicles as the criterion for determining the LOS (shown in **Table 2-6**), and the same criteria were used until the publication of the HCM7. The average density was computed using the total flow divided by the average space mean speed. The HCM2000 further revised the model by updating the constants for computation of the weaving intensity factors and the coefficient in the equation estimating the number of lanes required for the unconstrained condition(HCM, 2000). In addition, the HCM2000 updated the limitation of application for analysis of the weaving segments and added capacity estimation tables. The capacity was defined as any combination of flows that cause the density to reach LOS F, using the boundary density of 43 pc/ln/mi. Based on the configuration, the number of lanes, free flow speed (FFS), segment length, and volume ratio, the user could estimate the segment capacity. However, the capacity prediction did not impact the determination of the LOS.

Table 2-6: LOS criteria in HCM1997 (Transportation Research Board, 1997)**.**

Level of Service	Maximum Density (pc/mi/ln)	
	Freeway Weaving Area	Multilane and C-D Weaving Areas
A	10	12
B	20	24
C	28	32
D	35	36
E	≤43	≤40
F	>43	>40

After the HCM2000, the NCHRP 3-75 project was launched to develop a revised method in order to simplify model calibration as well as the consistency of predictions with other types of freeway segments (R. Roess & Uliero, 2008) The research was based on Fazio's speed estimation model (1985). To eliminate the need for determining the configuration type, Fazio recalibrated Reilly's model by adding lane change parameters (Fazio, 1985). The HCM2010 adopted NCHRP 3-75's approach (HCM, 2010). In the HCM2010, the speed of weaving and non-weaving was predicted based on the estimated lane changes. The following equations determine the weaving and non-weaving speeds (HCM2010):

$$S_{\mathrm{w}} = 15 + \frac{FFS - 15}{1 + W}$$

$$\text{where } W = 0.226\left(\frac{LC_{\mathrm{ALL}}}{L_{\mathrm{s}}}\right)^{0.789} \tag{2-2}$$

$$S_{\mathrm{nw}} = \mathrm{FFS} - (0.0072LC_{\mathrm{min}}) - \left(0.0048\frac{V}{N}\right) \tag{2-3}$$

In addition, the HCM2010 changed the method for predicting the segment capacity and estimated capacity to be the lower of the following two estimates:

$$c_{\mathrm{IWL}} = c_{\mathrm{IFL}} - [438.2(1 + VR)^{1.6}] + (0.765L_{\mathrm{s}}) + (119.8N_{\mathrm{wl}}) \tag{2-4}$$

$$c_{\mathrm{IW}} = \frac{2{,}400}{\mathrm{VR}}(for\ N_{\mathrm{wl}} = 2 \text{ lanes})$$

$$\text{or } \frac{3{,}500}{\mathrm{VR}}(for\ N_{\mathrm{wl}} = 3 \text{ lanes}) \tag{2-5}$$

where:

c_{IW} is the capacity (per lane) of the weaving segment under equivalent ideal conditions (pc/h/ln)

c_{IFL} is the capacity (per lane) of a basic freeway segment with the same FFS as the weaving segment under equivalent ideal conditions (pc/h/ln)

L_{s} is the short length of the weaving segment (ft)

N_{wl} is the number of lanes from which a weaving maneuver may be made with one or no lane changes.

Other variables are as previously defined.

Equation (5) estimates capacity based on density, while Equation (6) estimates capacity based on weaving demand. Moreover, the predicted capacity became an important factor in determining the final LOS. If the volume exceed capacity, then the traffic was considered to operate at LOS F.

2.2 Related Studies

Various macroscopic and microscopic models have been developed in addition to those included in various editions of the HCM. In 1963, Hess developed a regression-based model that used lane distribution to estimate the merge, diverge, and freeway volume in the auxiliary lane and the adjacent freeway lane (Hess, 1963). In 1983, Leisch independently recalibrated his 1965 Leisch-Norman model, however the concept and form of the model did not change significantly.

The first microscopic model was developed by Moscowitz and Newman (Moskowitz & Newman, 1962). The model defined the lane-changing distribution between the auxiliary lane and the adjacent freeway lane. However, the model tied the lane-changing distribution solely to the length of the segment. This model was then further calibrated in other studies undertaken between 1988 and 1995 (M. Cassidy et al., 1990; M. J. Cassidy & May, 1991; Ostrom et al., 1993; Windover & May, 1994). All these studies were funded by the California Department of Transportation (CALTRANS) and conducted by the University of California at Berkley. The calibrated models were all focused on lane changing in the rightmost lane of the freeway and auxiliary lanes. Those models were well-calibrated and provided far greater precision than the model by Moscowitz and Newman. However, the workload to calibrate the model for different sites was huge.

In the early 2000s, Lertworawanich and Elefteriadou introduced a methodology that used linear optimization and gap acceptance modeling to predict the weaving capacity (Lertworawanich, 2003; Lertworawanich & Elefteriadou, 2001, 2003). The methodology is theoretically rational, and the authors concluded that the ramp-to-freeway weaving demand affects operations more than the freeway-to-ramp weaving demand. However, the gap acceptance model in the methodology was based on an older gap acceptance model by Drew (Drew, 1965), and Raff and Hart(Raff & Hart, 1950). Therefore, the capacity estimates may need to be adjusted to consider current driver behavior and vehicle characteristics. In 2020 Mohajeri and Akbarzadeh evaluate the accuracy of different HCM methods based on Iranian drivers' behavior. They found that HCM 3rd Edition has best adaptation with the filed data for the speed of non-weaving vehicles, while HCM6 is best to estimate the rate of lane changings in the weaving sections. Also, they found that HCM 5th Edition is best to estimate the level of service for weaving sections(Mohajeri & Akbarzadeh, 2020).

In 2020, Dezhong Xu et al. proposed a new framework for modeling the speed of weaving segments. In this method, the speed in the weaving section is related to the speed in the equivalent basic segment. They calibrated four models to predict the speed within ramp weave sections(D. Xu et al., 2020). All of them outperformed the HCM model in terms of RMSE and R^2, but the combination of the performance metrics was the best for the last model (Eq-2-9).

$$S_o = S_b - 0.0579 * \text{FFS} * \left(\frac{\text{VR}}{L_s \text{ (in miles)}}\right)^{0.838} \quad (2\text{-}6)$$

$$S_o = S_b - 0.0555 \times \text{FFS} \times \left(\frac{V_{aux}}{V * L_s \text{ (in miles)}}\right)^{0.831} \quad (2\text{-}7)$$

$$S_o = S_b - 0.125 \times FFS \times \left(\frac{\frac{V_{rf}}{V}}{L_s \text{ (in miles)}}\right)^{0.455} \times \left(\frac{\frac{V_{fr}}{V}}{L_s \text{ (in miles)}}\right)^{0.409} \quad (2\text{-}8)$$

$$S_o = S_b - 0.109 \times \text{FFS} \times \left(\frac{\frac{V_{on-ramp}}{V}}{L_s \text{ (in miles)}}\right)^{0.515} \times \left(\frac{\frac{V_{off-ramp}}{V}}{L_s \text{ (in miles)}}\right)^{0.370} \quad (2\text{-}9)$$

While these models generally work well, they provide some counterintuitive results because they estimate increasing speeds when the through or non-weaving volume increases without an increase in weaving traffic. In 2021 Amini et al. proposed new mathematical models that solve this issue. However, the model that they proposed was designed and calibrated for type A weave sections and couldn't evaluate weave sections type B and C (Amini et al., 2021).

2.3 Literature Evaluating the HCM7 Weaving Analysis Method

Even though the weaving segment operational analysis method in the HCM6 was updated relatively recently, some studies have found that the speed and capacity models are not accurate. Field data collected from 93 sites in California showed that the HCM6 over-predicted the density by 8% for balanced weaving segments and by 24% for unbalanced weaving segments (Alexander Skabardonis & Mauch, 2015). Additional Bluetooth and video-recorded data revealed that the method over-predicted the density by an average of 13.4%. The researchers did a follow-up study using data collected from Athens, Greece(Alexander Skabardonis et al., 2016). The follow-up study showed that the HCM6 overestimated density by 17% for situations where the volume ratio (*VR*) was high. These studies also concluded that the HCM6 underestimates the capacity of weaving segments, especially in cases where the *VR* is high.

The possible causes of these discrepancies are that the HCM6 overemphasizes the impact of the *VR*, and that it uses a high value of the basic freeway segment capacity. A study based on field observations of capacity revealed that the observed basic freeway capacity is significantly lower than the recommended number in the HCM (Kondyli et al., 2017). In addition, several studies have questioned the assumption of using a density of 43 pc/mi/ln to estimate the weaving segment capacity (Lertworawanich & Elefteriadou, 2001, 2003, 2007). They found this density assumption has not been justified in the literature and there are no data to validate it.

The HCM6 speed models have also been criticized. Zhou (Zhou et al., 2015) found that, compared to field data, the HCM6 weaving speed prediction has an error as high as 40% for some scenarios. In addition, the study found that in some cases, the predicted weaving speed is higher than the predicted non-weaving speed, which is counterintuitive. Another study found that the HCM6 speed estimation has low sensitivity to the weaving segment length(Ahmed et al., 2019). The authors found that the average space mean speed only increased by 7% when the segment length

was quadrupled, even with high levels of weaving demands. This occurs because the non-weaving lane change model does not include the segment length as a variable. Kashani, Shirgir in 2021 conducted a sensitivity analysis on the boundary situation for the maximum length of weaving sections. They compared two different scenarios. First when the length of weaving section is equal to maximum length of weaving section (based on the HCM6, if the length of weaving section is greater than the maximum length of weaving sections it should be considered as a separate on ramp and off ramp segments). Second, when a merge segment is followed by a diverge segment and the sum of the acceleration and deceleration of these two segments is equal to the maximum length of weaving section. In these boundery situations the performance for two sections should be the same. However, they found that based on density and speed analysis, the separate merging and diverging segments perform better than the weaving segment with equal length and traffic volume(Kashani & Shirgir, 2021b). Also Kashani, Shirgir in 2021 found that the calculation of maximum length of weaving sections can be improved by replacing VR with Three new variables (F_{fr} ($\frac{V_{fr}}{V_{ff}}$), F_{rf} ($\frac{V_{rf}}{V_{rr}}$), and FR ($\frac{V_{rf}}{V_{rf}}$)) (Kashani & Shirgir, 2021a).

In summary, the literature review showed that the HCM6 method needs further improvement regarding the accuracy of capacity estimation models, speed estimation models, and consistency with the performance estimates for basic freeway segments. In addition, the models are not as sensitive to the geometric characteristics of the sites as field data indicate.

3. DATA COLLECTION

This research aims to improve the capacity prediction model for weaving segments (Type A) proposed in an earlier study by the authors (Rouphail et al., 2021) as well as test a new set of speed prediction models for major weaves (Types B and C). The speed model forms for major weaves tested here are tied to the ramp weave speed model developed in Phase I. We collected observational data from 14 Type B and six Type C weaving segments. The necessary data elements can be divided into geometric and traffic operational traits. According to the previously developed model, the geometric data include the weaving segment length and lane configuration (as explained later). Those are readily available for any location from satellite views of Google Maps or Google Earth. Conversely, collecting traffic operation data such as traffic speed and total and weaving flow rates must be gathered from field surveys.

The team had access to several archived databases of observational data from weaving segments across the US. However, most of those fell into Type A (ramp weaves) and Type B (one class of major weaves) weaves. Therefore, the team carried out field surveys to collect additional data for Type C (also major) weaves. The next section describes the data elements observed from each site and a short description of the selected sites. The following two sections describe the traffic data collection and extraction techniques adopted in the field surveys for Type C weaves and the data sources for Type B weaves. Finally, the need for removing inconsistent data points and a technique for that are demonstrated.

3.1. Data Elements and Site Description

Traffic data at each site were aggregated in 5-minute intervals. Tables 3-1 and 3-2 list all Type B and Type C sites, respectively, along with their geometric characteristics and the number of 5-minute observations extracted from each. All Type C weaves are located within or near Raleigh, NC. Data elements regarding traffic operational characteristics include flow rates by origin-destination routes and overall average speed of traffic. Data elements regarding geometric characteristics are shown below. The potential importance of these characteristics to the proposed model are described in Chapter 4.

Short length (in ft): Distance between the end points of any barrier markings (solid white lines) that prohibit or discourage lane changing (see HCM7 for definition)

Number of lanes (N): Total number of lanes in a weaving segment (including the auxiliary lane(s))

LC_{RF} and LC_{FR}: The minimum number of lane changes required by a ramp-to-freeway (LC_{FR}) and a freeway-to-ramp vehicle (LC_{FR})

N_{wRF} *and* N_{wFR} *:* The number of lanes from which a ramp-to-freeway or freeway-to-ramp maneuver can be completed in no or at most one lane change.

The total number of data points for Type B and C weaves was 19,547 and 96. Note that there is a significant imbalance of number of data points for these two types of weaves, which is due to the availability of archived data from the former type.

Table 3-1: Listing of type B weaving segments and their attributes

Location	Short length (ft)*	Number of Lanes	LC_{RF}	LC_{FR}	N_{wRF}	N_{wFR}
2100 s Fwy@ Bangerter Hwy	1230	4	1	0	1	2
2100 s Fwy@ Belt route	1381	4	1	0	1	2
Bayshore Fwy@ Ralstio Ave	1670	5	1	0	1	2
veterans memorial hwy @ Center St	1860	6	1	0	1	2
veterans memorial hwy @ Antelope De Dr	2313	4	1	0	1	2
veterans memorial hwy @ 700 South	2316	4	1	0	1	2
veterans memorial hwy @ Orem 1600 N	2438	6	1	0	1	2
veterans memorial hwy @ 800 North	2484	6	1	0	1	2
veterans memorial hwy @ 5300 south	2657	5	1	0	1	2
veterans memorial hwy @ Center St	2966	6	1	0	1	2
veterans memorial hwy @ Antelope Dr	2982	4	1	0	1	2
veterans memorial hwy @ 12300 South	3136	5	1	0	1	2
veterans memorial hwy @ Belt Route	3425	5	1	0	1	2
veterans memorial hwy @ Lakeview Pkwy	3494	5	1	0	1	2

Table 3-2: Listing of type C weaving segments and their attributes

Location	Number of 5-minute observations	Short length (ft)*	Number of Lanes	LC_{RF}	LC_{FR}	N_{wRF}	N_{wF}
I-440 WB between Poole Rd & I-87	15	1,628	5	2	0	0	2
I-87 EB between I-440 & New Hope Rd	37	2,722	4	0	2	2	0
I-40 WB between I-540 & Page Rd	20	2,995	6	0	2	2	0
I-440 WB between New Bern Ave & Brentwood Rd	8	3,250	5	0	2	2	0
US-1 NB between Tryon Rd & SE Cary Pkwy	19	3,614	4	0	2	2	0
I-40 EB between N Harrison Ave & Wade Ave	19	5,597	5	2	0	0	2

3.2. Traffic Data Collection for Type C Weaves

Field surveys were conducted for collecting data from Type C weaves since not many archived data were found for this type of weaves. The feasibility of collecting origin-destination-based traffic data was in important criterion for selecting the study sites. Our primary data collection methods were drone mounted videos cameras. To extract data from the videos, we used both manual re-identification as well as an automated vehicle tracking tool (DataFromSky, 2022). The automated tool was described in detail in earlier research (Rouphail et al., 2021). The main limitation of the camera is that it can only cover up to 1,700 ft of a straight segment when mounted on a drone. Both FAA regulations on the maximum altitude of a drone, and --for the extraction process-- the minimum size of the vehicles in the frame required by the automated vehicle tracking tools— contributed to this limitation. The coverage length is much shorter of course for ground-based cameras. To work around this problem, we used ground cameras supplemented by a drone-mounted camera or Bluetooth sensors to collect route-based flow rate data. As we show in the next subsection, a combination of ground and drone cameras gives the most accurate estimate of route-based flow rates for long weaves. Hence, we adopted this approach in four of the six data collection sites. The short length (see Chapter 13 of HCM7 for definition) at one of the sites is 1,628 ft, so one drone-mounted camera was sufficient at that location. We used Bluetooth sensor data from the remaining site which we collected for a previous project (Rouphail et al, 2020). A new survey was conducted with a ground camera to supplement the Bluetooth data.

The team used the average speed data reported by RITIS (Ritis, 2022) for five of the six sites. RITIS estimates the average travel time for a segment at a time interval from the GPS pings of a sample of the vehicles (known as probes). For the short site (which was surveyed by a single camera), we estimated the travel time of individual vehicles with the help of DataFromSky.

The following subsections describe these data collection and reduction methods.

Using Drone-based and Ground-based Cameras

We classify the flow rates into two types, namely, (a) the flow rate at a particular location and (b) that for an origin-destination across a weaving segment. The flow rate at a location can be measured by installing a camera targeting that section. However, measuring the origin-destination based flow rates requires re-identifying or tracking individual vehicles through a pair of locations. Our target was to do the least amount of re-identification, since manually doing so is a very time-consuming process. Note that vehicle tracking is not feasible using this method if the entire segment cannot be covered by a single video camera.

The first step of the process was to measure the flow rates at the four origins and destinations of a weave, namely, freeway upstream, on-ramp, freeway downstream, and off-ramp. Flow rates at these borders at any timestep (*i*) are represented by $V_i^{FWY,US}$, V_i^{ONR}, $V_i^{FWY,DS}$, and V_i^{OFR}, respectively, and are illustrated in Figure 3-1. These flow rates can be obtained from video

records at any of the three out of the four boundaries. The remaining flow rates can be calculated from the conservation of flow equation.

$$V_i^{\mathrm{FWY,US}} + V_i^{\mathrm{ONR}} = V_i^{\mathrm{FWY,DS}} + V_i^{\mathrm{OFR}}. \qquad \text{Eq. 3-1}$$

There are four origin-destination flow rates, namely, freeway-to-freeway (V^{FF}), freeway-to-ramp (V^{FR}), ramp-to-freeway (V^{RF}), and ramp-to-ramp (V^{RR}). With the flow rates at each of the locations known, only one origin-destination flow rate is needed to calculate the rest. We first assume that V^{RR} is known (which is generally the lowest flow among the four and hence, requires the least number of re-identifications). Equations 3-2 through 3-4 show how to calculate the rest.

$$V_i^{\mathrm{RF}} = V_i^{\mathrm{ONR}} - V_i^{\mathrm{RR}}. \qquad \text{Eq. 3-2}$$
$$V_i^{\mathrm{FF}} = V_i^{\mathrm{FWY,DS}} - V_i^{\mathrm{RF}}. \qquad \text{Eq. 3-3}$$
$$V_i^{\mathrm{FR}} = V_i^{\mathrm{FWY,US}} - V_i^{\mathrm{FF}}. \qquad \text{Eq. 3-4}$$

Thus, the manual task narrows down to measuring V^{RR}, which one could accomplish by matching vehicles captured by the ground cameras at the on and off ramps (see Figure 3-1). In this Figure, the drone is capturing $V^{\mathrm{FWY,US}}$, but one could fly it over the downstream end to capture $V^{\mathrm{FWY,DS}}$.

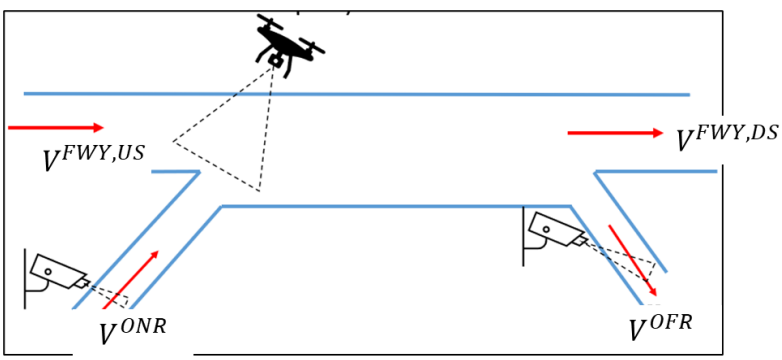

Figure 3-1: Data collection mechanism for long (short length > 1,700 ft) weaves using ground and drone cameras

This technique has a few drawbacks. First, the process is complex and requires several instruments to be operating simultaneously. Matching the timestamps of all three cameras is very critical. Moreover, as mentioned earlier, manual re-identification takes a long time (about eight hours to process one-hour video for lightly trafficked ramps). Nonetheless, this technique provides the most accurate estimate of the origin-destination flow rates for a weave.

Using Bluetooth sensors and ground cameras

The manual re-identification part of the process described above would be difficult to employ when the ramp flow rates are high. However, if the ratio of the merging and diverging traffic (i.e.,

$\frac{V^{\mathrm{RF}}}{V^{\mathrm{ONR}}}$ and $\frac{V^{\mathrm{FR}}}{V^{\mathrm{FWY,US}}}$, respectively) are known, the process can be cut down to measuring only the denominators (i.e., V^{ONR} and $V^{\mathrm{FWY,US}}$). Alternatively, one would only need V^{OFR} and $V^{\mathrm{FWY,DS}}$ if $\frac{V^{\mathrm{FR}}}{V^{\mathrm{OFR}}}$ and $\frac{V^{\mathrm{FF}}}{V^{\mathrm{FWY,DS}}}$ were known.

The research team estimated these ratios for a Type C weave (located at I-40 EB between North Harrison Avenue and Wade Avenue near Raleigh, NC) for a past project by deploying a Bluetooth sensor at each border. The ramp traffic flow rates at this weave were higher than the other Type C weaves in this area (Source: NCDOT AADT Webmap (Ncdot, 2022)). A Bluetooth sensor can detect the MAC IDs of the Bluetooth-enabled units for a fraction of vehicles in a traffic stream. We estimated $\frac{V^{\mathrm{FR}}}{V^{\mathrm{OFR}}}$ using the following equation:

$$\left(\widehat{\frac{V^{\mathrm{FR}}}{V^{\mathrm{OFR}}}}\right) = \frac{M^{\mathrm{FR}}}{D^{\mathrm{OFR}}}. \qquad \text{Eq. 3-5}$$

Here, $\widehat{V^{\mathrm{FR}}/V^{\mathrm{OFR}}}$ is an estimate of $\frac{V^{\mathrm{FR}}}{V^{\mathrm{OFR}}}$, M^{FR} is the number of matches between the Bluetooth sensors at the upstream freeway and the off-ramp boundaries, and D^{OFR} is the total number of detections at the off-ramp boundary.

The calculation of its counterpart ratio followed the same process.

The Bluetooth sensors collected field data from 4 pm to 6 pm on three consecutive weekdays—June 11 to June 13, 2019. We estimated the average ratios across these multiple days. Data on V^{OFR} and $V^{FWY,DS}$were collected more recently (on October 10, 2022) from the same site at the same clock time (4 pm-6 pm) using ground cameras. The underlying assumption was that the proportions for those hours did not change significantly between the two dates. We then entered the flow rates for each timestamp *i* and the ratios to the following equations to estimate the weaving flow rates:

$$\widehat{V_i^{\mathrm{FR}}} = \left(\widehat{\frac{V^{\mathrm{FR}}}{V^{\mathrm{OFR}}}}\right) * V_i^{\mathrm{OFR}}. \qquad \text{Eq. 36}$$

$$\widehat{V_i^{\mathrm{RF}}} = \left(\widehat{\frac{V^{\mathrm{RF}}}{V^{\mathrm{FWY,DS}}}}\right) * V_i^{\mathrm{FWY,DS}}. \qquad \text{Eq. 3-7}$$

3.3. Data Sources for Type B Weaves

We obtained data from 14 Type B weaving segments from which were collected using loop detectors. The main consideration for site selection was to have at least four loop detectors at each side (at on ramp, offramp, freeway upstream side and freeway downstream side). The data were collected on September 12–18, 2019, in 5-min time intervals (2,016 data points for each site). We assumed that 5% of the traffic consist of heavy vehicles (as suggested by HCM7 for the

percentage of heavy vehicles on urban freeways) and converted all flow rate values to passenger car equivalents accordingly. The observed traffic flow rate ranged from 4 to 1,805 pc/h/ln.

To estimate each of the four traffic flows in the weaving sections using detector data, we developed a new method (called proportional method) which assumes that the proportion of the weaving flow rates relative to the total flow rate remains the same. In this method, we have defined a new variable called exiting proportion (EP) which can be calculated as:

$$EP = \varphi \times \frac{V^{OFR}}{V^{\mathrm{FWY,US}} + V^{\mathrm{ONR}}}. \qquad \text{Eq. 3-8}$$

Then the four-traffic flows will be calculated as:

$$V^{RR} = EP \times V^{ONR} \qquad \text{Eq. 3-9}$$

$$V^{FR} = V^{RR} - V^{OFR} \qquad \text{Eq. 3-10}$$

$$V^{FF} = V^{FWY,US} - V^{FR} \qquad \text{Eq. 3-11}$$

$$V^{RF} = V^{ONR} - V^{RR} \qquad \text{Eq. 3-12,}$$

Where,

φ is a model parameter;

The rest of variable have been explained before.

To estimate the value of φ, eight Type B weave sections from NCHRP database (Roess et al., 2008) were selected. Then we used Generalized Reduced Gradient (GRG) nonlinear optimization to minimize the average magnitude of relative error (MRE) between models' prediction and observed data over all four flows. The result of the optimization shows that the minimum value of average MRE (14.06) will be when α is equal to 1.91. Figure 3-2 show the observed vs predicted flow for the weaving maneuvers when the value of α is equal to 1.91.

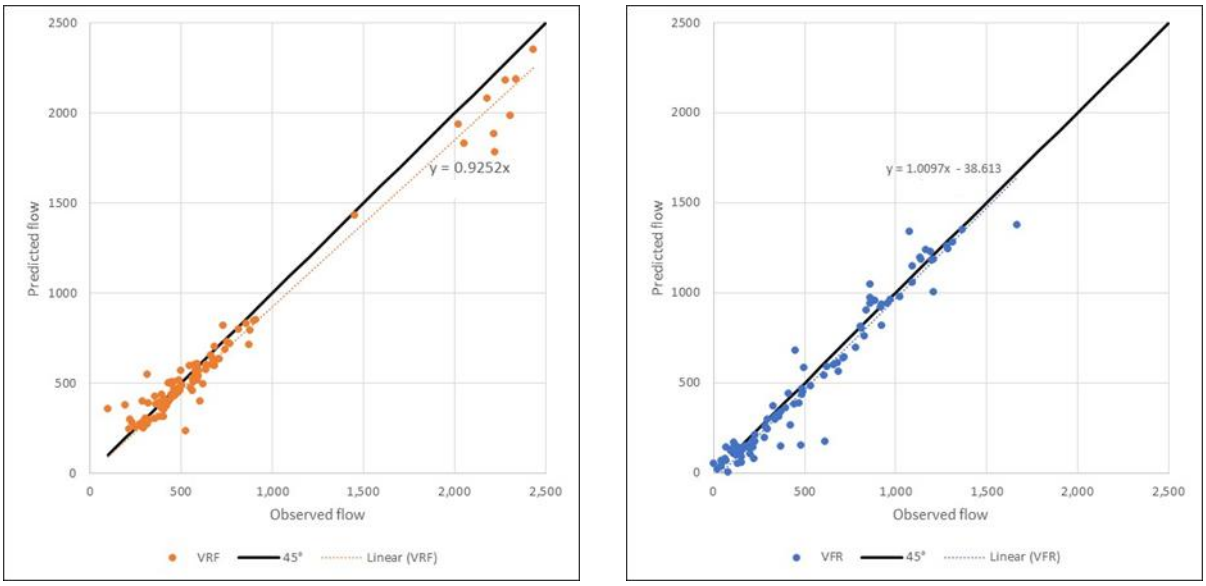

(a) (b)

Figure 3-2: Observed vs predicted value of weaving maneuvers; (a) is for V^{RF} and (b) is for V^{FR} (ϕ = 0.91)

This proportional method was used to estimate the four traffic flows in the weaving sections when the data is collected using loop detectors.

3.4. Data Filtering

Since the model development is data driven, it is important to remove inconsistent and mixed state data traffic data from the raw database. Figure 3-3 shows the raw speed-flow data for the Veterans memorial Highway at Antelope De Drive. It contains many low-density observations (i.e., low flow rate in the uncongested regime) for which the speed was unexpectedly low. Such observations exist due to inclement weather, work zones, incidents, or any other sort of capacity drop phenomena as well as from observations that include both congested and uncongested flow.

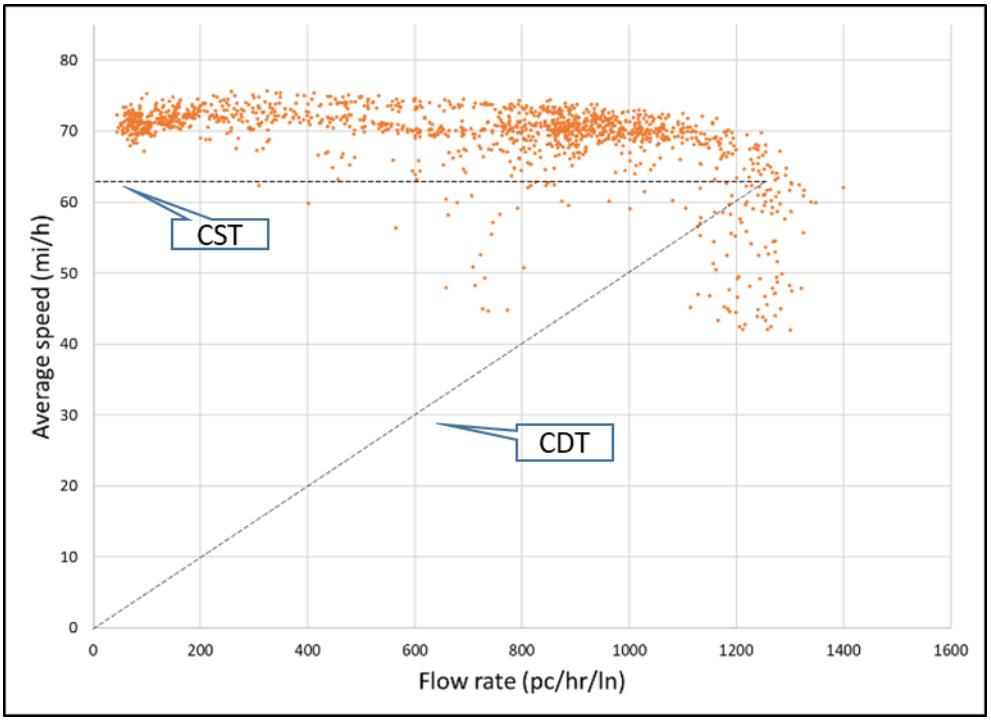

Figure 3-3: Identifying inconsistent data points from speed-flow graph for a Type B weave

To remove such observations, we adopted a modified version of a macroscopic traffic data filtering technique proposed by Xu et al. (Y. Xu et al., 2013). It involves two thresholds, namely, Critical Speed Threshold (CST) and Critical Density Threshold (CDT). The combined application of these two thresholds removes the low-speed observations associated with low volume. CST is used to identify low speed (congested) observations. Analysis of traffic data reveals that 10 mph below the speed limit (the horizontal dashed line in Figure 3-3) is a reasonable threshold to determine congested observations. CDT is used to identify low volume observations. A density of 20 pc/mi/ln is defined as the CDT threshold (shown by the oblique dashed line in Figure 3-3). Observations that fall below both CST and CDT thresholds are tagged as inconsistent (low-speed and low-volume) data points. These data points, bounded by the two dashed lines, are removed from further analyses.

This filter removed 486 observations from the Type B database. The importance of the data cleaning process warrants to re-develop the Type A model using the cleaned data, which was originally developed in the previous study on ramp weave led by the authors. Originally, the dataset for Type A weaves included 14,067 data points from 15 sites. Data from two sites were removed as their quality seemed to be questionable. Upon applying the two thresholds on the data from the remaining 13 sites, the final dataset included 9,228 observations.

4. METHODOLOGY

This chapter describes the methodological details of the proposed speed model and adjustments to the capacity model for weaving segments. The first section demonstrates how the speed model developed earlier for Type A weaves is modified to model all three types of weaves. The second section shows how the capacity model, which is linked to the speed model, is adjusted to reflect the changes in the speed model. Additional adjustments to the capacity model that address a critical limitation are also discussed at the end of the chapter.

4.1. Proposed Speed Model for All Types of Weaves

In a previous study, we proposed the following model form to estimate the overall mean speed for **Type A** weaves.

$$S_o = S_{\mathrm{b}} - \mathrm{SIW}, \qquad \textit{Equation 4-1}$$

where,

S_o = overall mean speed for all vehicles in the weaving segment (mi/h);

S_{b} = mean speed for all vehicles in an equivalent basic segment with the same number of lanes *N,* same total demand volume *v* (pc/h), and same free-flow speed FFS (mi/h). We estimated this term following HCM7.

SIW = speed impedance term due to weaving and segment configuration (mi/h). It accounts for the turbulence due to weaving, and is a function of weaving demands, total flow rates, number of lanes, and segment length. The final equation for SIW that was fitted for Type A weaves is shown below. For flow rate per lane less than 500, $SIW = 0$.

$$\mathrm{SIW} = \alpha * \left(\frac{\beta * v_{\mathrm{rf}} + v_{\mathrm{fr}}}{N}\right)^{\gamma} \times \left(\frac{v}{N} - 500\right) \times \left(\frac{1}{L_s}\right)^{\delta}, \qquad \textit{Equation 4-2}$$

where,

v_{rf} = ramp-to-freeway demand flow rate in the weaving segment (pc/h);
v_{fr} = freeway-to-ramp demand flow rate in the weaving segment (pc/h);
v = total demand flow rate in the weaving segment (pc/h);
L_s= the short length (ft) of the weaving segment;
$\alpha, \beta, \gamma, and\ \delta$ are model coefficients.

For most Type A weaves, one lane change is required by both ramp-to-freeway and freeway-to-ramp weaving traffic. Hence, there is no need to include any lane configuration parameter other than the total number of lanes. Conversely, the lane configuration for Type B and C weaves may strongly influence their operating condition. Shared thru-exit and exclusive exit lanes affect the weaving maneuvers' complexity (or comfort) in different ways. Hence, the proposed model includes in the SIW equation lane configuration parameters for each weaving traffic: the minimum number of lane changes required for the ramp-to-freeway and freeway-

to-ramp traffic ($\mathrm{LC_{rf}}$ and $\mathrm{LC_{fr}}$, respectively) and the number of lanes from which a weaving maneuver can be completed with no more than one lane change (N_{wrf} and N_{wfr}). The updated form of SIW is:

$$\mathrm{SIW} = \alpha * \left(\frac{\frac{v_{\mathrm{rf}} * (\mathrm{LC_{rf}}+1)}{\mathrm{N_{wrf}}+1} + \frac{v_{\mathrm{fr}} * (\mathrm{LC_{fr}}+1)}{\mathrm{N_{wfr}}+1}}{N^{\varepsilon}} \right)^{\gamma} * \left(\frac{v}{N} - 500 \right) * \left(\frac{1}{L_{\mathrm{s}}} \right)^{\delta}, \qquad \textit{Equation 4-3}$$

where, ε is the exponent coefficient for the number of lanes and all other parameters are explained above.

As shown, this equation does not include the coefficient that determines the relative weight of the ramp-to-freeway and freeway-to-ramp flow rates since the lane configuration variables account for that.

Table 4-1 shows several weaving configurations for major weaves located in the US with different N, $\mathrm{LC_{rf}}$, $\mathrm{LC_{fr}}$, N_{wrf}, and N_{wfr} values.

In the updated equation of SIW, a higher value for LC indicates a more complex weaving maneuver with added turbulence to the through traffic, whereas a higher value for N_{w} would reduce it.

Although this model form can be fitted to data that include all three types of weaves, the research team developed separate models for ramp weaves (i.e., Type A) and major weaves (i.e., Type B and C). During the calibration process, it was determined that the difference in lane configuration between ramp and major weaves might cause the other factors to affect traffic speed differently. One could also develop separate models for Type B and C weaves if sufficient data for each type are available.

Table 4-1: Different lane configurations for Type B and C weaving segments

Location	Type	Geometric configuration	N	N_{wrf}	N_{wfr}	$\mathrm{LC_{rf}}$	$\mathrm{LC_{fr}}$
I-85 WB between Hillandale Rd & US-501, NC	C	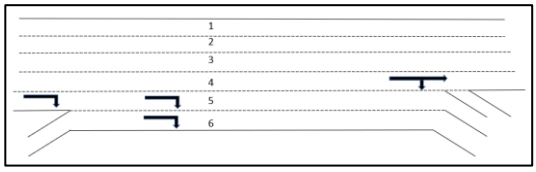	6	0	3	2	0
I-440 NB between Poole Rd & I-85, NC	C	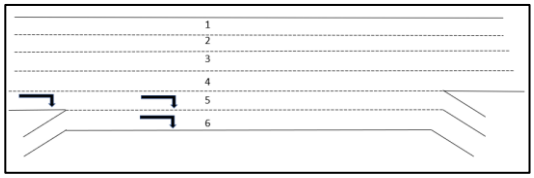	6	0	2	2	0
I-85 EB between US-501 & Hillandale Rd, NC	C	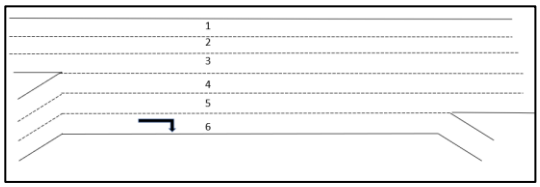	6	3	0	0	3
SR 102 WB between Tatum Blvd & SR 51, AZ	B	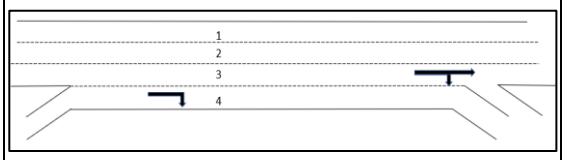	4	1	2	1	0

4.1.1. Speed Model Development

In order to calibrate these models, the root-mean-square error (RMSE) was used as a criterion for obtaining the model parameters through the optimization process.

MSE is obtained as:

$$MSE = \frac{1}{n}\sum_{i=1}^{n}(Y_i - \overline{Y_i})^2. \qquad \textit{Equation 4-4}$$

Where:

Y_i is the predicted speed;
$\overline{Y_i}$ is the observed speed;
n is the number of data points.

Generalized reduced gradient (GRG) nonlinear optimization was used to minimize the value of RMSE between the predicted speed and observed speed. To keep the parameters in a reasonable and valid range, we set constraints on each coefficient minimum and maximum value. Through trial-and-error, we made sure that these constraints had little effect on the value of RMSE. The optimization model is of the following form:

$$Objective\ function: minimize\ MSE$$

$$s.t., 0.2\ \leq \alpha, \delta, \varepsilon, and\ \gamma\ \leq 20$$

Error! Reference source not found. presents the estimated parameters for the proposed model (Equation 4-3) for both major and ramp weaves. The value of RMSE for the model is also presented in this table.

Table 4-2: Parameters estimation for models 13-15

Coefficients	Ramp weave	Major weave
α	20*	20*
δ	0.79	1.12
γ	0.44	0.40
ε	10.19	3.85
Model RMSE (mi/h)	***2.36***	***3.46***

**Values are at the boundary of the constrain*

4.1.2. Speed Model Validation

Key geometric features that impact weaving operations include the short length (L_s) of the weaving section as well as the number of lanes. We expect that a weaving section with long L_s would yield a higher speed than a section with short L_s. Therefore, the variable L_s should be a denominator term in SIW. On the other hand, increasing the number of lanes (N) provides non-weaving vehicles more opportunities to increase their speed by moving to a non-weaving lane and avoiding the conflict area (i.e., the area of the weaving section extending from the rightmost auxiliary lane to the lane directly to the left of the diverge gore (Alex Skabardonis & Kim, 2010). Conversely, fewer lanes would result in lower speeds within the weaving section. Therefore, the number of lanes should also be a denominator term in SIW.

Total traffic volume has a varying relation with speed. At very low volumes, and regardless of the amount of weaving traffic, speed in the weaving section is expected to be similar to the equivalent basic freeway segment. Under those conditions, there are adequate gaps so that even at a relatively moderate volume, weaving movements can complete their maneuvers at their desired speed. As traffic volume increases, however, a low number of weaving vehicles can cause a drop in speed. The field data collected in this study have confirmed this general trend.

4.2. Capacity Model

In this section, the capacity model form proposed in an earlier study led by the researchers is adjusted to reflect the changes in the speed model. A modified form of the model, which was spurred from a critical limitation of its current form, is introduced toward the end of this chapter.

4.2.1. Initial Model

The capacity estimation procedure proposed in the earlier study is connected to speed estimation because it must satisfy the fundamental traffic flow equation. The equation can be derived by evaluating the speed at capacity in Equation 4-1. This equation can be rewritten as Equations 4-5 and 4-6 for speed at capacity:

$$S_0^{\mathrm{c}} = \frac{C_{\mathrm{w}}}{k_{\mathrm{w}}^{\mathrm{c}}} = S_{\mathrm{b}}^{\mathrm{c}}(C_{\mathrm{w}}, C_{\mathrm{w}}^2) - \mathrm{SIW} \qquad \textit{Equation 4-5}$$

where,

S_0^{c}= overall average speed when the weaving segment is at capacity (mi/h);

C_{w} = weaving segment capacity (pc/h/ln);

$k_{\mathrm{w}}^{\mathrm{c}}$ = density of the weaving segment at capacity (pc/mi/ln);

$S_{\mathrm{b}}^{\mathrm{c}}(C_{\mathrm{w}}, C_{\mathrm{w}}^2)$ = basic segment speed evaluated at the weaving segment capacity (mi/h).

Chapter 12 of the HCM7 proposed the following equation for estimating the basic segment speed at C_{w}.

$$S_{\mathrm{b}}(C_{\mathrm{w}}, C_{\mathrm{w}}^2) = \mathrm{FFS} - \left(\mathrm{FFS} - \frac{C_{\mathrm{b}}}{k_{\mathrm{w}}^{\mathrm{c}}}\right) * (C_{\mathrm{w}} - \mathrm{BP})^2/(C_{\mathrm{b}} - \mathrm{BP})^2, \qquad \textit{Equation 4-6}$$

See the HCM7 for the definitions and equations for:

BP = basic segment breakpoint (pc/h/ln) and

C_{b} = equivalent per-lane basic segment capacity (pc/h/ln).

If we assume that the observed weaving flow rates (v_{rf} and v_{fr}) remain the same while the total flow rate reaches capacity from v, Equation 4-5 becomes a quadratic equation of C_{w} and can be solved analytically. Equations 4-7 and 4-8 show the derivation of the quadratic form of C_{w} . Note that this assumption is likely to be invalid when the observed flow rate is substantially lower than the capacity. In the following subsection, we will show how we can avoid this somewhat unrealistic assumption. Based on the above assumption, Equation 4-5 can be written as:

$$\frac{C_{\mathrm{w}}}{k_{\mathrm{w}}^{\mathrm{c}}} = S_{\mathrm{b}}(C_{\mathrm{w}}, C_{\mathrm{w}}^2) - \alpha * \left(\frac{\frac{v_{\mathrm{rf}}*(\mathrm{LC_{rf}}+1)}{\mathrm{N_{wrf}}+1} + \frac{v_{\mathrm{fr}}*(\mathrm{LC_{fr}}+1)}{\mathrm{N_{wfr}}+1}}{N^{\varepsilon}}\right)^{\gamma} * (C_w - 500) * \left(\frac{1}{L_{\mathrm{s}}}\right)^{\delta}. \qquad \textit{Equation 4-7}$$

Rearranging Equation 4-7 to a quadratic function of C_{w} yields Equation 4-8:

$$a * C_{\mathrm{w}}^{2} + b * C_{\mathrm{w}} + d = 0. \qquad \textit{Equation 4-8}$$

Here, $= \; k_{\mathrm{w}}^{\mathrm{c}} * \frac{\left(\mathrm{FFS} - \frac{C_{\mathrm{b}}}{45}\right)}{(C_{\mathrm{b}} - \mathrm{BP})^{2}}$;

$b = \; 1 + k_{\mathrm{w}}^{\mathrm{c}} * \mathrm{W} - 2 * \mathrm{a} * \mathrm{BP}$;

$d = a * \mathrm{BP}^{2} - 500 * k_{\mathrm{w}}^{\mathrm{c}} * \mathrm{W} - k_{\mathrm{w}}^{\mathrm{c}} * \mathrm{FFS}$;

$$W = weaving\ segment\ intensity = \alpha * \left(\frac{\frac{v_{\mathrm{rf}} * (\mathrm{LC}_{\mathrm{rf}} + 1)}{N_{\mathrm{wrf}} + 1} + \frac{v_{\mathrm{fr}} * (\mathrm{LC}_{\mathrm{fr}} + 1)}{N_{\mathrm{wfr}} + 1}}{N^{\varepsilon}} \right)^{\gamma} * \left(\frac{1}{L_{\mathrm{s}}} \right)^{\delta}.$$

The HCM7 and its predecessors assumed that the density at capacity ($k_{\mathrm{w}}^{\mathrm{c}}$) for any weaving segment is a fixed value of 43 pc/mi/ln. However, we showed in the previous chapter that field observations from many sites suggest that it is substantially lower than that. We used $k_{\mathrm{w}}^{\mathrm{c}} = 35\ pc/mi/ln$ in this study, but it can be even lower for some sites.

4.2.2. Alternate Model to Account for Weaving Ratios

Despite the analytical flexibility of the quadratic form of Equation 4-8, the underlying assumption that the observed weaving flow rates will remain the same at capacity makes it somewhat unrealistic. This assumption can be far from reality if the observed flow rate is significantly lower than the segment's capacity. In this project, we replaced this assumption with a more realistic one, that is, the *ratio* of the observed weaving flow rates to the total flow rate (the variable VR in the HCM7) remains constant. We assume that the total and weaving flow rates at capacity are $\mu * v, \mu * v_{\mathrm{rf}}\ and\ \mu * v_{\mathrm{fr}}$, respectively, where μ is an unknown multiplication factor. Equation 4-9 is the companion version of Equation 4-7 with this new assumption. Solving it for μ would consequently estimate the per lane weaving segment capacity as $C_w = \mu * \frac{v}{N}$.

$$\frac{\mu * v}{N * k_{\mathrm{w}}^{\mathrm{c}}} = \mathrm{S_b}\ (\mu * v, \mu^{2} * v^{2}) - \alpha * \left(\frac{\frac{v_{\mathrm{rf}} * \mu * (\mathrm{LC}_{\mathrm{rf}} + 1)}{N_{\mathrm{wrf}} + 1} + \frac{v_{\mathrm{fr}} * \mu * (\mathrm{LC}_{\mathrm{fr}} + 1)}{N_{\mathrm{wfr}} + 1}}{N^{\varepsilon}} \right)^{\gamma} * \left(\mu * \frac{v}{N} - 500 \right) \times \left(\frac{1}{L_{\mathrm{s}}} \right)^{\delta}. \qquad \textit{Equation 4-9}$$

This equation does not have a closed-form solution given the various exponents in the different terms in the model. However, it can be solved numerically via a simple search method that minimizes the differences between its left- and right-hand sides. In general, that revised capacity will be slightly lower than the one estimated using Equation 4-8 since it assumes that both the total and weaving flow rates increase to reach the capacity.

The ultimate choice of the capacity model should be based on the required accuracy, the observed flow rates, and the availability of a numerical analysis tool. As the observed flow rate (v) becomes close to the capacity, the difference between the two models diminishes significantly. Compared to Equation 4-9, Equation 4-8 is perhaps easier to solve for many users,

but as cautioned earlier, it may overestimate the capacity if the observed flow rate is low. In the next chapter, we will demonstrate the application of both models through an example problem and show that under most "relevant" moderate to congested flow conditions, the simplified capacity estimate using the quadratic Equation 4-8 works quite well.

5. RESULTS

This chapter presents the results from developing and testing the proposed speed and capacity models to enable capacity analyses for weaving segments. The first part of the chapter discusses the speed models developed. Following that, the chapter illustrates the sensitivity of the segment capacity as a function of several critical model variables. Lastly, the proposed methods are applied to an example problem for a Type B weave from the HCM7 to compare the speed and capacity estimates between the proposed and the existing method.

5.1. Average Speed Model

As mentioned in previous chapters, two models are developed: one for Type A or ramp weaves and another for Type B and C, i.e., major or complex weaves. The estimated coefficient values, the quality of the model fit, and the resulting speed-flow characteristics are discussed below. The speed model is rewritten here for clarity purposes. All the symbols are explained in Chapter 4.

$$S_{\mathrm{o}} = S_{\mathrm{b}} - \alpha * \left(\frac{\frac{v_{\mathrm{rf}} * (\mathrm{LC_{rf}} + 1)}{\mathrm{N_{wrf}} + 1} + \frac{v_{\mathrm{fr}} * (\mathrm{LC_{fr}} + 1)}{\mathrm{N_{wfr}} + 1}}{N^{\varepsilon}} \right)^{\gamma} * \left(\frac{v}{N} - 500 \right) * \left(\frac{1}{L_{\mathrm{s}}} \right)^{\delta} \qquad \textit{Equation 5-1}$$

5.1.1. Model Coefficients

Table 5-1 shows the estimated coefficient values and the root-mean-squared error (RMSE) of the ramp and major weaves model.

Table 5-1: Speed model for ramp (Type A) and major (Type B and C) weaves

Coefficients	Ramp weave	Major weave
α	20*	20*
δ	0.79	1.12
γ	0.44	0.4
ε	10.19	3.85
Model RMSE (mi/h)	2.36	3.46

**value at the boundary of the constraints used in the model development*

As mentioned in section 4.1.1, all coefficients are constrained between 0.2 and 20. The estimated value of α for both weaves is at the upper boundary, implying that had it not been bounded it would probably go beyond and further reduce the RMSE. However, the constraints are selected based on a trial-and-error process, which indicated that the reduction in RMSE is marginal when α exceeds this limit.

The remaining coefficient values are different for the two weave types, although, except for ε, the difference between the two models is low. δ, the negative exponent for segment length, is

higher for major weaves. Referring to Eq. 4-3, it indicates that the impact of segment length on average speed is stronger for major weaves than for ramp weaves. ε , the coefficient for number of lanes is significantly higher for ramp weaves. Note that the exponent for number of lanes is, in fact, $(-\gamma * \varepsilon)$, which is, respectively, -4.48 and -1.54 for ramp and major weaves. Hence, according to this model, the impact of number of lanes on the estimated speed is more substantial for ramp weaves than for major weaves.

5.1.2. Quality of Model Fit

Table 5-1 shows that the model RMSE for major weaves is slightly higher than that for ramp weaves; however, both are less than 3.5 mi/h. Therefore, the overall model error is deemed acceptable. For a more detailed investigation, we plotted the fitted and observed speed data in Figures 5-1 (a) and 5-1 (b) for ramp and major weaves, respectively. The fitted value is equal to the observed value along the diagonal line. Figure 5-1 (c) and Figure 5-1 (d) are their counterparts for the test data.

The distribution of the data points with respect to this line is almost symmetric for Type A weaves when the observed speed is higher than 60 mi/h. For the remaining region, the high concentration of data above the diagonal line indicates over-estimation by the model at low-speed conditions. Thus, the model is primarily driven by high-speed observations for both types of weaves because most of the data are in that speed region.

For major weaves, the data distribution is almost symmetric with respect to the diagonal when the observed speed is higher than 55 mi/h. However, for lower speeds, it is even more imbalanced than that for ramp weaves. In fact, there is a cluster (marked by the red oval in Figure 5-1 (b) of observations for which the predicted speed is around 60 to 78 mi/h, whereas the observed speed varies between 40 to 55 mi/h. We could not find any documented unique geometric features of the sites associated with this cluster. These data could be related to some unique traffic operational characteristics (e.g., incident or weather induced flow disruption) for which the observed speed was low but the model could not capture that.

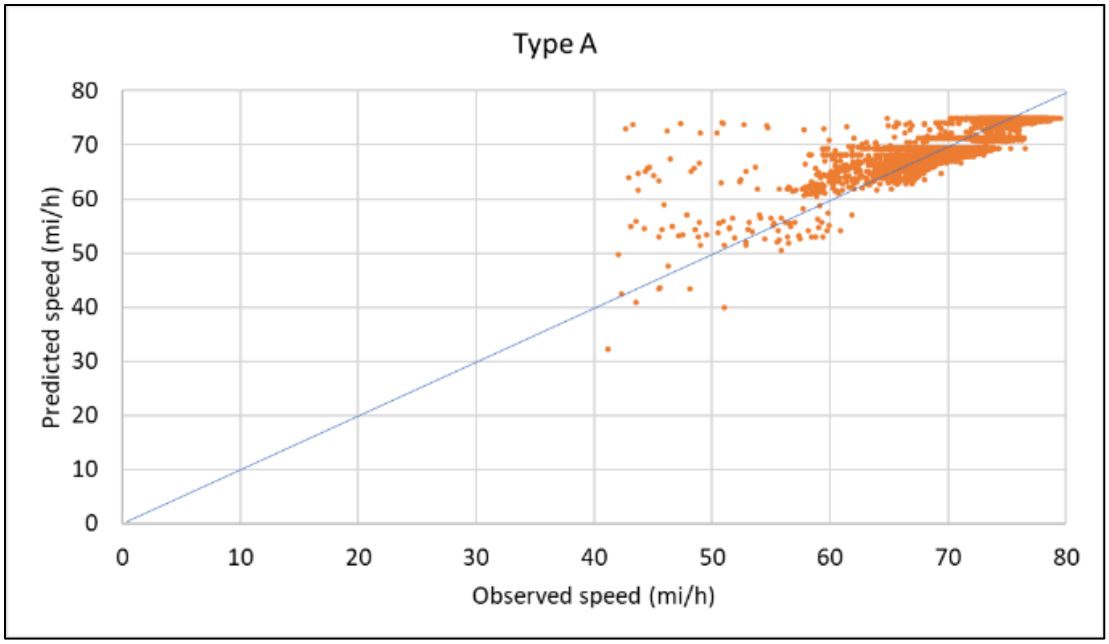
Type A
Predicted speed (mi/h)
Observed speed (mi/h)
0
10
20
30
40
50
60
70
80

(a)

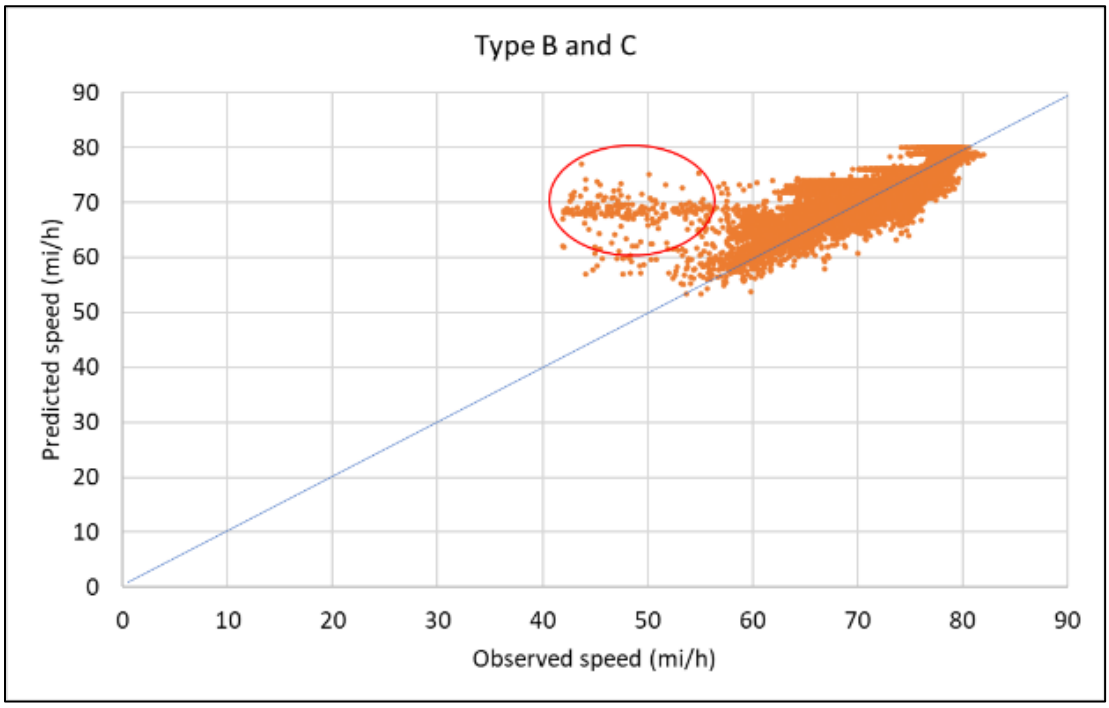
Type B and C
Predicted speed (mi/h)
Observed speed (mi/h)
0
10
20
30
40
50
60
70
80
90

(b)

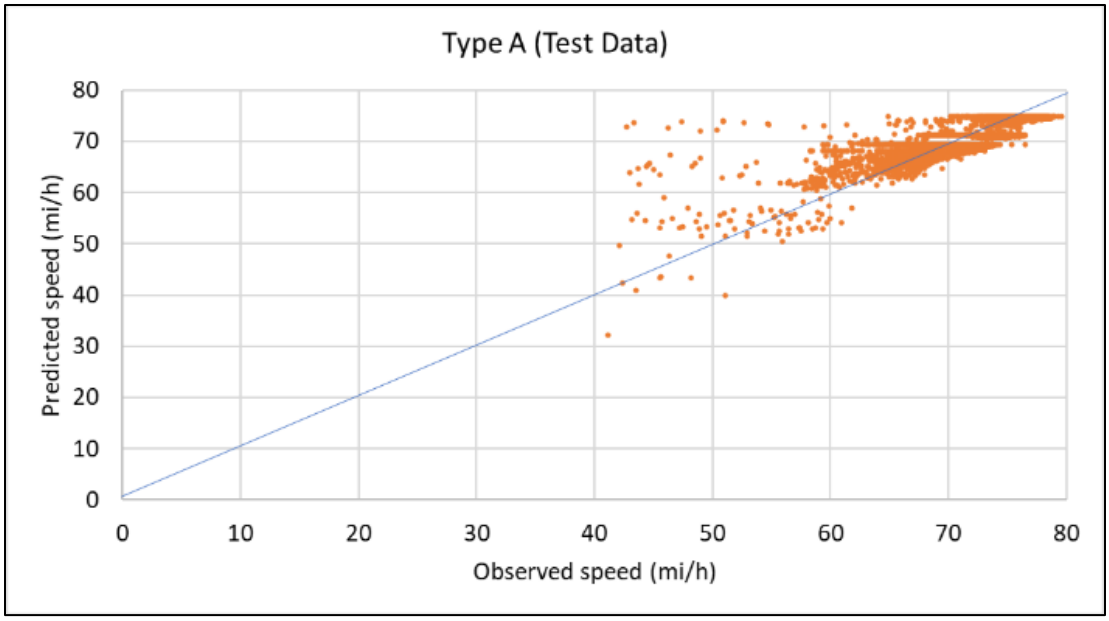

(c)

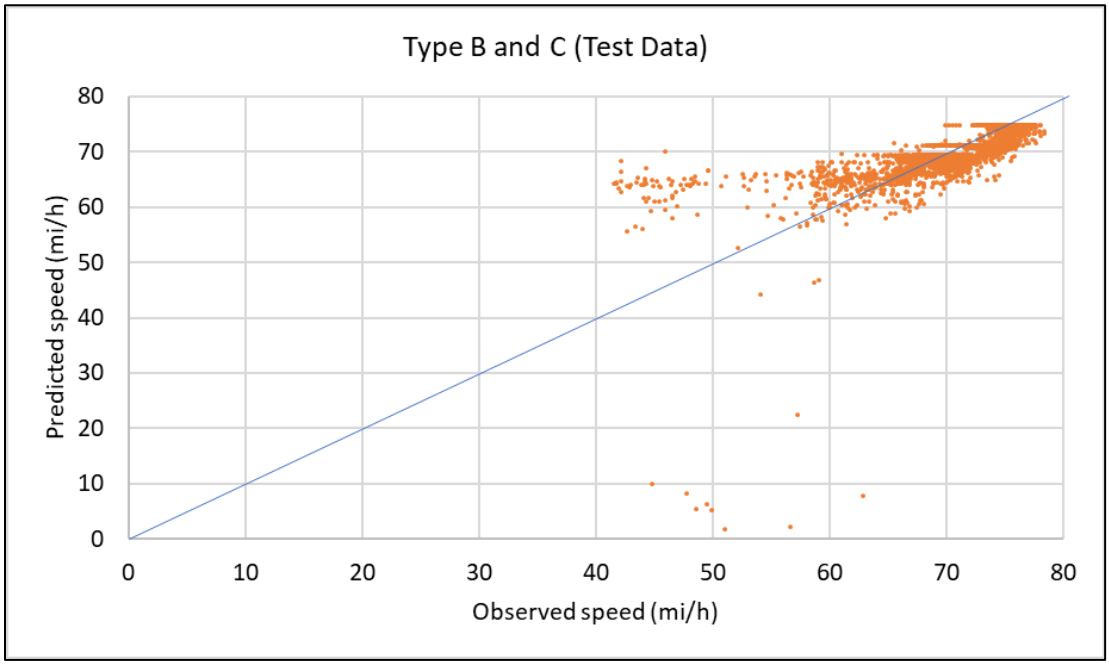

(d)

Figure 5-1: Predicted vs observed average speed for (a) training data for ramp weaves (Type A), (b) training data for major weaves (Type B and C), (c) test data for ramp weaves, and (d) test data for major weaves

To test the developed models, we separated 20% of the data for each weaving type which were not used in the model development stage. The calibrated model was applied to that test dataset. Figure 5-1 (c) and Figure 5-1 (d) show the results for ramp and major weaves, respectively. The resulting RMSE for the test dataset was 2.56 and 4.70 mi/h. Similar to the model development RMSE, the test data RMSE for major weaves is higher than that for ramp weaves. However, it is

noteworthy that the model performed poorly for a small fraction of observations in the major weave test data. Nonetheless, the test results are deemed satisfactory since the resulting RMSE is not substantially higher than the model calibration RMSE.

5.1.3. Speed-Flow Characteristics

Figure 5-2 shows the observed speed-flow diagram overlaid with the predicted speed data. Traffic density is constant at 35 pc/mi/ln on the oblique line. Up to flow rate = 500 pc/hr/ln, the predicted speed is equal to the free flow speed of the corresponding site. The speed starts to drop beyond 500 pc/hr/ln for both types of weaves. However, no speed drop is visible for some ramp weave sites until the flow rate reaches 1,200 pc/hr/ln. Conversely for major weaves, most data points show a visible speed drop between 500 and 750 pc/hr/ln flow rate.

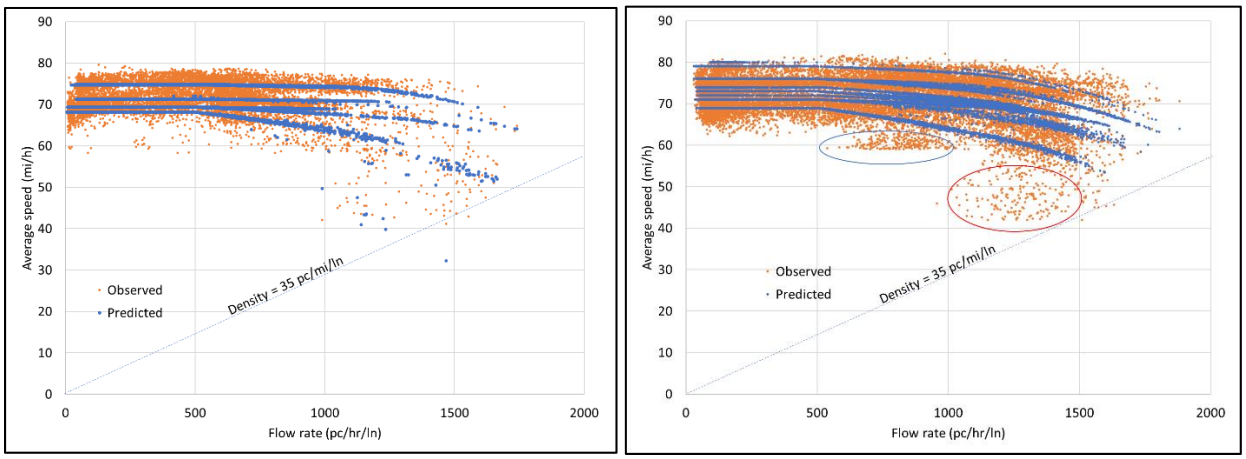

(a) (b)

Figure 5-2: Speed-flow diagram for (a) ramp (Type A) and (b) major (Type B and C) weaves

The highest observed flow rate for ramp and major weaves is 1,740 and 1,880 pc/hr/ln, respectively. The highest observed density is about 35 pc/mi/ln for both types. Beyond that value, the traffic state was congested (note: congested data are not shown in Figure 5-2). Thus, no observation was found to reach the breakdown density that HCM7 currently uses (43 pc/mi/ln). For major weaves, the cluster of poorly fitted data shown in Figure 5-1 (b), is also visible in Figure 5-2 (b). The corresponding observed flow rate is between 1,000 to 1,500 pc/hr/ln and the speed is between 40 to 55 mi/h. Furthermore, marked by the blue oval is another cluster for which the speed is also surprisingly low, given the flow rate is between 500 and 1,000 pc/hr/ln. This cluster is not easily discernible from Figure 5-1 (b) since the difference with the predicted speed is low. Such low speeds when the flow rate is not close to the capacity for a site are typically attributed to unusual events like inclement weather or lane blockage due to construction or accidents. This observation remarks the need for manually removing those data.

5.2. Sensitivity of Capacity

In this section, numerical experiments were performed to compare the sensitivity of the proposed and the HCM7 capacity models for major weaves to the critical geometric and traffic

variables like segment length, weaving ratio, and total number of lanes. Note that the variables related to lane change requirements might also be critical to capacity, but they can take only a few sets of values. Moreover, major weaves are usually (if properly) designed in a way that the higher of the two weaving flow rates is required to make the least number of lane changes. Therefore, it would be impractical to consider some unrealistic combinations of weaving flow rates and lane change requirements. In all sensitivity cases, the segment free flow speed was set at 65 mph.

The proposed capacity models provided in Chapter 4 are repeated below for reference. Equation 5-2 is analytically solvable for capacity (C_w), whereas Equation 5-3 needs to be solved for the ratio of the capacity to observed flow rate (μ) through a series of numerical iterations. Of the two HCM7 capacity models, Equation 5-4 shows the one that dictates in most practical cases (it also governs in the scenarios considered here).

$$\frac{C_{\mathrm{w}}}{k_{\mathrm{w}}^{\mathrm{c}}} = S_{\mathrm{b}}(C_{\mathrm{w}}, C_{\mathrm{w}}^2) - 20 * \left(\frac{\frac{v_{\mathrm{rf}}*(\mathrm{LC_{rf}}+1)}{\mathrm{N_{wrf}}+1} + \frac{v_{\mathrm{fr}}*(\mathrm{LC_{fr}}+1)}{\mathrm{N_{wfr}}+1}}{N^{3.85}}\right)^{0.4} * (C_w - 500) * \left(\frac{1}{L_s}\right)^{1.12}. \qquad \textit{Equation 5-2}$$

$$\frac{\mu * v}{N * k_{\mathrm{w}}^{\mathrm{c}}} = \mathrm{S_b}\ (\mu * v, \mu^2 * v^2) - 20 * \left(\frac{\frac{v_{\mathrm{rf}}*\mu*(\mathrm{LC_{rf}}+1)}{N_{\mathrm{wrf}}+1} + \frac{v_{\mathrm{fr}}*\mu*(\mathrm{LC_{fr}}+1)}{N_{\mathrm{wfr}}+1}}{N^{3.85}}\right)^{0.4} * \left(\mu * \frac{v}{N} - 500\right) \times \left(\frac{1}{L_s}\right)^{1.14}. \qquad \textit{Equation 5-3}$$

$$C_w = C_{IFL} - 438.2 * (1 + VR)^{1.6} + (0.0765 * L_s) + (119.8 * N_{WL}), \qquad \textit{Equation 5-4}$$

where,

$C_{IFL} =$ capacity (per lane) of a basic freeway segment with the same FFS as the weaving segment under equivalent ideal conditions (pc/h/ln);

$VR =$ ratio of weaving to total flow rate;

$N_{WL} =$ Number of lanes from which a weaving maneuver can be completed with no more than one lane change. The remaining symbols are explained earlier.

We varied the value of segment length, number of lanes, and weaving ratio individually and estimated the capacity for each case. Figures 5-3 through 5-5 show the resulting diagrams. When one variable is changed, the fixed values for the rest are shown in these figures.

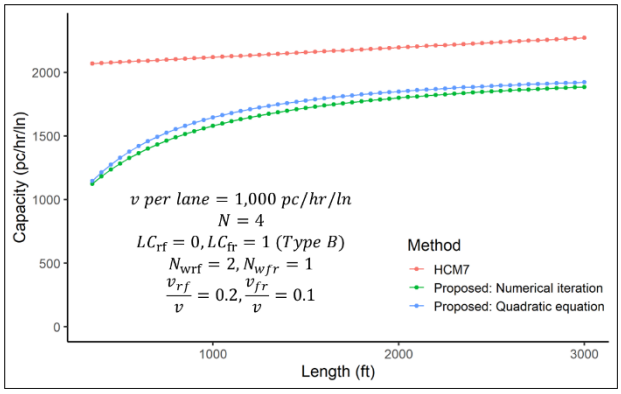

Figure 5-3: Sensitivity of weaving capacity to segment length

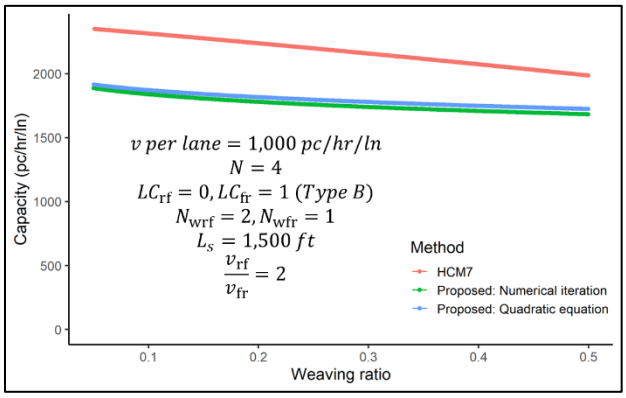

Figure 5-4: Sensitivity of weaving capacity to weaving ratio

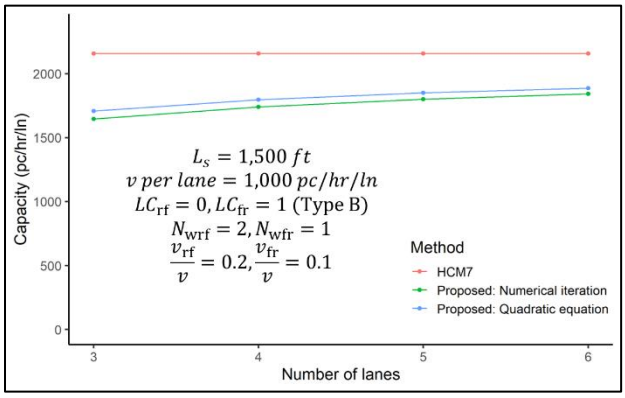

Figure 5-5: Sensitivity of weaving capacity to number of lanes

A general observation from the above figures is that the HCM7 model persistently estimated a capacity greater than 2,000 pc/hr/ln regardless of the geometric and traffic characteristics. It is substantially higher than the proposed models' estimates as well as observations from the field data. Another prevalent observation is that the difference in capacity estimated by the two proposed models is negligible for all cases, i.e., they practically generate very similar results.

As apparent in Figure 5-3, the HCM7 model exhibits a weak sensitivity to segment length, whereas the two proposed models are remarkably sensitive, particularly when the segment

length is below 1,000 ft. On the other hand, the HCM7 model shows a slightly higher sensitivity to weaving ratio than the proposed models (Figure 5-4). The reason is that the HCM7 model is directly linked to weaving ratio, as shown in Equation 5-5. The proposed models estimated a somewhat higher per lane capacity as the number of lanes goes from 3 to 4, but overall, they show minimal sensitivity to this variable. The HCM7 model shows no sensitivity to the number of lanes as per Equation 5-4.

5.3. HCM7 Example Problem

We applied the proposed speed and capacity estimation procedures to an example problem for Type B weaves in HCM7 (Chapter 27, Problem #1) to compare and assess our results against the HCM7 estimates of speed and capacity. Figure 5-3 shows the schematic of the corresponding weaving segment.

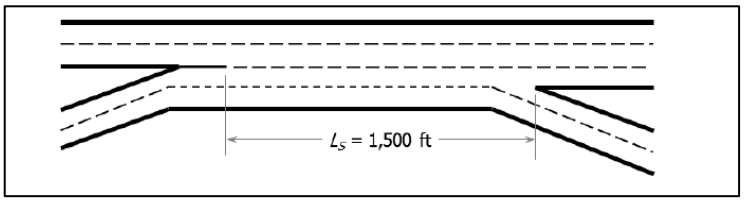

Figure 5-6: Schematic of the site in Problem 1 of Chapter 27 in HCM7

Below are the input parameters.

Geometric Properties:
Short length, $L_s = 1{,}500\ ft$;
Free flow speed, $\mathrm{FFS} = 65\ mi/hr$;
Number of lanes, N = 4;
Minimum number of lane changes required for ramp-to-freeway traffic, $\mathrm{LC_{rf}} = 0$;
Minimum number of lane changes required for freeway-to-ramp traffic, $\mathrm{LC_{fr}} = 1$;
Number of lanes from which a ramp-to-freeway maneuver can be completed with no more than one lane change, $N_{\mathrm{wrf}} = 2$;
Number of lanes from which a freeway-to-ramp maneuver can be completed with no more than one lane change, $N_{\mathrm{wfr}} = 1$.

Traffic Flow Properties:
Ramp-to-freeway flow rate, $v_{\mathrm{rf}} = 1{,}197\ pc/hr/ln$;
Freeway-to-ramp flow rate, $v_{\mathrm{fr}} = 798\ pc/hr/ln$;
Total flow rate, $v = 5{,}586\ pc/hr$.

Equations 5-2 and 5-3 are the numerical models for average speed and capacity, respectively, for major weaves developed in this study. Here, the capacity is estimated by solving Eq. 5-3 for μ using a non-linear optimization technique, which minimizes the difference between the two sides of the equation, and multiplying that by $\frac{v}{N}$

$$S_o = 65 - 20 * \left(\frac{1{,}197 * \frac{0+1}{2+1} + 798 * \frac{1+1}{1+1}}{4^{3.85}} \right)^{0.4} \times \left(\frac{5{,}586}{4} - 500 \right) \times \left(\frac{1}{1{,}500} \right)^{1.12}.$$

Equation 5-2

$$\frac{\mu * 5{,}586/4}{35} = S_b \left(\mu * \frac{5{,}586}{4}, \mu^2 * 5{,}586^2/4^2 \right) - 20 * \left(\frac{\frac{1{,}197 * \mu * (0+1)}{2+1} + \frac{798 * \mu * (1+1)}{1+1}}{4^{3.85}} \right)^{0.4} \times \left(\mu * \frac{5{,}586}{4} - 500 \right) \times \left(\frac{1}{1{,}500} \right)^{1.12}.$$

Equation 5-3

Table 5-2 shows the speed and capacity estimated by HCM7 and the model developed for major weaves in this study.

Table 5-2: Speed and capacity for the example problem for a major weave in HCM7

Outputs	HCM7	Proposed method ($computed\ \mu = 1.226$)
Average speed (mi/h)	53.1	55.0
Capacity (pc/hr/ln)	2,001	1,712
Volume-to-capacity ratio	0.70	0.81

The average speeds estimated by the two methods are very similar. However, the HCM7 method estimates a significantly higher capacity than the proposed method, which resulted a lower volume-to-capacity ratio. For a speed observation that is about 12 mi/h lower than the free flow speed, a volume-to-capacity ratio of 0.7 seems to be unrealistically low. Moreover, the capacity estimated by HCM7 is significantly higher than what we observed in the field (maximum capacity for a Type B site was 1,880 pc/hr/ln). Hence, although the speed estimates do not differ much, the proposed method estimated a more realistic capacity value than the HCM7.

6. SUMMARY, CONCLUSIONS, AND RECOMMENDATIONS

6.1. Summary

The objectives of this study were to develop improved models estimating the average speed and capacity for major weaves (i.e., Type B and Type C). The basic form of the speed model followed the one developed by the research team for ramp weaves (aka Type A weaves). We incorporated two lane-configuration parameters for each type of weaving traffic to formulate a generic model form for all three types of weaving segments. These are: the minimum number of lane changes required for the ramp-to-freeway and freeway-to-ramp traffic ($\mathrm{LC_{rf}}$ and $\mathrm{LC_{fr}}$, respectively) and the number of lanes from which a weaving maneuver can be completed with no more than one lane change (N_{wrf} and N_{wfr}). The recommended models directly estimate the average segment speed using the equivalent basic segment speed minus a weaving turbulence speed impedance term (SIW). Similar to the ramp weave speed model the proposed models ensure consistency with the basic freeway segment, avoid the need to predict the number of lane changes, and separately estimate weaving and non-weaving flow speeds, which are extremely difficult to calibrate in the field.

The final speed models for both types of weaves are shown below.

Major weave speed (Types B and C):

$$S_{\mathrm{o}} = S_{\mathrm{b}} - 20 * \left(\frac{v_{\mathrm{rf}} * \frac{\mathrm{LC_{rf}}+1}{\mathrm{N_{wrf}}+1} + v_{\mathrm{fr}} * \frac{\mathrm{LC_{fr}}+1}{\mathrm{N_{wfr}}+1}}{N^{3.85}} \right)^{0.4} \times \left(\frac{v}{N} - 500 \right) \times \left(\frac{1}{L_{\mathrm{s}}} \right)^{1.12}.$$

The data for Type B weaves were obtained from archived loop detectors at 14 multi-state sites around the US. A simple yet effective and validated technique called the "*proportional weaving method*" was used to estimate weaving flow rates from loop detectors installed at all approaches of a weave. Due to the lack of archived data for Type C weaves, new field surveys were conducted using drone-mounted and ground cameras at six sites in North Carolina. The data were then extracted using a combination of manual matching and automated counting using a computer vision-based tool. The final dataset for major weaves included 19,158 five-minute-aggregated observations, 80% of which were used to develop the model, while the remainder was used for testing.

This new set of speed models was used to formulate the capacity model. The capacity equation previously proposed by the researchers for Type A weaves was based on the assumption that the observed weaving flow rates remain the same as the total flow rate reaches capacity. The equation below is the resulting model for major weaves formulated based on this approach. In this case, a closed form solution using a quadratic equation can be used to predict capacity.

Previous model (major weaves):

$$\frac{C_{\mathrm{w}}}{35} = S_{\mathrm{b}}(C_{\mathrm{w}}, C_{\mathrm{w}}^2) - 20 * \left(\frac{\frac{v_{\mathrm{rf}} * (\mathrm{LC_{rf}}+1)}{\mathrm{N_{wrf}}+1} + \frac{v_{\mathrm{fr}} * (\mathrm{LC_{fr}}+1)}{\mathrm{N_{wfr}}+1}}{N^{3.85}} \right)^{0.4} * (C_w - 500) * \left(\frac{1}{L_s}\right)^{1.12}$$

In this project, we replaced this assumption with a more realistic one, that is, the ***ratio*** of the observed weaving flow rates to the total flow rate (the variable VR in the HCM7) remains constant. However, the resulting equation, shown below, has no closed-form solution. Instead, it needs to be solved numerically via multiple iterations for the ratio of the capacity to the observed flow rate (μ), where $\mu = \frac{N * C_W}{v}$.

Proposed model (major weaves):

$$\frac{\mu * \frac{v}{N}}{35} = \mathrm{S_b}\left(\mu * \frac{v}{N}, \mu^2 * \frac{v^2}{N^2}\right) - 20 * \left(\frac{\frac{v_{\mathrm{rf}} * \mu * (\mathrm{LC_{rf}}+1)}{N_{\mathrm{wrf}}+1} + \frac{v_{\mathrm{fr}} * \mu * (\mathrm{LC_{fr}}+1)}{N_{\mathrm{wfr}}+1}}{N^{3.85}} \right)^{0.4} * \left(\mu * \frac{v}{N} - 500\right) * \left(\frac{1}{L_s}\right)^{1.12}.$$

However, it should be noted that the difference in the capacity estimates from these two approaches are meaningful only when the observed flow rate is low; it diminishes as the observed flow rate approaches capacity. Note that unlike the HCM7 method, which incorporates two capacity models, the models developed by the researchers are based on a single equation. Thus, the closed form capacity model is recommended for all applications for all practical purposes.

Finally, the breakpoint density observed in the field data was substantially lower than the Phase I and the HCM7 models used (43 pc/mi/ln). Field data suggested densities less than or equal to 35 pc/mi/ln are valid, thus their use in both capacity estimation methods. All the symbols in the equations shown here are explained in detail in Chapter 4.

6.2. Conclusions

Below are the key findings from this study.

- The resultant root-mean-squared error (RMSE) for the predictive speed models were 3.46 and 2.36 mi/h, respectively, for major and ramp weaves. They attest that the overall fit was more than acceptable. The application of the models to the corresponding test/ validation dataset not used in the model development also yielded satisfactory RMSE values—4.7 mi/h for major and 2.56 mi/h for ramp weaves.
- Since the data from Type C weaves represented only a small fraction of the entire major weave database, we applied the major weaves' speed model only to Type C data to test its applicability to Type C weaves. The resulting RMSE was even lower than the model development RMSE.
- Despite showing an overall satisfactory fit, both speed models overestimated field speeds for a cluster of low-speed observations. An examination of the speed-flow scatter plots revealed that these observations have unexpectedly low speed given that the flow rate was less than 1,500 pc/h/ln and density between 10–35 pc/mi/ln. These data could be related to some unique traffic operational characteristics (e.g., incidents or weather-

induced flow disruptions) for which the observed speed was low, but the model could not capture those effects.

- The highest observed flow rate for ramp and major weaves was 1,740 and 1,880 pc/hr/ln, respectively. The highest observed density is about 35 pc/mi/ln for both types; beyond that, the traffic state was congested. Thus, no observation was found to reach the breakdown density that the HCM7 currently uses (43 pc/mi/ln).
- We tested the sensitivity of the two proposed capacity models and the HCM7 model to segment length, number of lanes, and weaving ratio. The HCM7 model showed minimal sensitivity to segment length, whereas the two proposed models were remarkably sensitive, particularly when the segment length is below 1,000 ft. However, the HCM7 model showed a slightly higher sensitivity to weaving ratio than the proposed models. None of the models showed a notable sensitivity to number of lanes.
- Both the proposed and the HCM7 weave analysis methods were applied to an example problem for a Type B weave. Although all the models generated similar speed drops (10-12 mi/h), the HCM7 model estimated a very high capacity (2,001 pc/hr/ln). The resulting volume-to-capacity ratio was thereby very low (0.70) for such a speed drop. Conversely, the capacity and v/c generated by the proposed models were within the anticipated range (1,720 pc/hr/ln and 0.80, respectively).

6.3. Recommendations for Future Research

The following are recommendations for future research:

- Sensor data obtained for this research are relatively easy to obtain in large quantities. However, such data do not guarantee that the flow breakdowns observed represent recurrent congestion conditions. Therefore, it is imperative to filter out observations associated with downstream bottlenecks, crashes, incidents (e.g., work zones), and inclement weather prior to model development. Such information can be obtained from public agencies and fused with sensor data.
- There should be a balance in the number of observations from different traffic states (e.g., free flow and near-capacity states). However, it was challenging to observe near-capacity states at many sites, particularly with a temporary camera as the data collection device. In this regard, permanent loop detectors are a better choice despite their inability to observe traffic origins and destinations.
- Although the density at the breakpoint is treated as a constant, field data suggests that it varied across sites from 22 to 35 pc/mi/ln. These changes could be attributed to the varying lane change rates for different sites at capacity and need to be investigated in future research. This observation also warrants an investigation of the breakpoint density for basic segments, for which the HCM7 suggests a fixed value of 45 pc/mi/ln.

7. REFERENCES

Ahmed, I., Rouphail, N. M., & Tanvir, S. (2018). Characteristics and temporal stability of recurring bottlenecks. Transportation Research Record, 2672(42), 235–246.

Ahmed, I., Xu, D., Rouphail, N., & Karr, A. (2019). Lane change rates at freeway weaving sites: trends in HCM6 and from NGSIM trajectories. Transportation Research Record, 2673(5), 627–636.

Amini, E., Xu, D., Rouphail, N. M., Elefteriadou, L., & Aghdashi, B. (2021). Capacity Analysis Framework for Freeway Ramp Weaves. Journal of Transportation Engineering, Part A: Systems, 147(12), 4021085.

Cassidy, M., Chan, P., Robinson, B., & May, A. D. (1990). A Proposed Analytical Technique for the Design and Analysis of Major Freeway Weaving Sections. Final Report.

Cassidy, M. J., & May, A. D. (1991). Proposed analytical technique for estimating capacity and level of service of major freeway weaving sections. Transportation Research Record, 1320, 99–109.

datafromsky. (2022). https://datafromsky.com/.

Drew, D. R. (1965). Gap acceptance characteristics for ramp-freeway surveillance and control. Texas Transportation Institute, Texas A & M University.

Fazio, J. (1985). Development and testing of a weaving operational design and analysis procedures. Master's Thesis, University of Illinois at Chicago, Chicago IL.

HCM. (1950). Highway capacity manual: Practical applications of research. US Department of Commerce, Bureau of Public Roads.

HCM. (1985). Special Report 209: Highway Capacity Manual. In Washington D.C.:Transportation Research Board, National Research Council.

HCM. (2000). Highway Capacity Manual 2000. In Washington D.C.: Transportation Research Board, National Research Council.

HCM. (2010). Hgihway Capacity Manual. Washington DC: Transportation Research Board.

HCM7. (2022). Highway Capacity Manual 7th Edition. Transportation Research Board, National Research Council, Washington, DC.

Hess, J. W. (1963). Traffic Operation in Urban Weaving Areas. Bureau of Public Roads (1963 Data, in Preparation for Publication).

Kashani, A., & Shirgir, B. (2021a). Development of maximum weaving length model based on HCM 2016. Transportation Research Record, 2675(4), 135–145.

Kashani, A., & Shirgir, B. (2021b). Sensitivity Analysis of Maximum Weaving Length for One-Sided Weaving Section Based on HCM 2016. Journal of Transportation Engineering, Part A: Systems, 147(1), 4020143.

Kondyli, A., George, B. S., Elefteriadou, L., & Bonyani, G. (2017). Defining, measuring, and modeling capacity for the highway capacity manual. Journal of Transportation Engineering, Part A: Systems, 143(3), 4016014.

Lertworawanich, P. (2003). Capacity estimation for weaving areas based on gap acceptance and linear optimization. Pennsylvania State University.

Lertworawanich, P., & Elefteriadou, L. (2001). Capacity estimations for type B weaving areas based on gap acceptance. Transportation Research Record, 1776(1), 24–34.

Lertworawanich, P., & Elefteriadou, L. (2003). A methodology for estimating capacity at ramp weaves based on gap acceptance and linear optimization. Transportation Research Part B: Methodological, 37(5), 459–483.

Lertworawanich, P., & Elefteriadou, L. (2007). Generalized capacity estimation model for weaving areas. Journal of Transportation Engineering, 133(3), 166–179.

Mohajeri, A., & Akbarzadeh, M. (2020). Appraisal of different HCM methodologies for analysis of weaving segments, case study: a weaving segment in Isfahan, Iran. Transportation Letters, 12(6), 408–416.

Moskowitz, K., & Newman, L. (1962). Notes on freeway capacity. California Division of Highways.

NCDOT. (2022). https://ncdot.maps.arcgis.com/apps/webappviewer/index.html?id=964881960f0549de8c3583bf46ef5ed4.

Normann, O. K. (1957). Operation of weaving areas. Highway Research Board Bulletin, 167, 38–41.

Ostrom, B., Leiman, L., & May, A. D. (1993). Suggested procedures for analyzing freeway weaving sections. Transportation Research Record, 42.

Raff, M. S., & Hart, J. W. (1950). A Volume Warrant for Stop Signs. Eno Foundation for Highway Traffic Control. Saugatuck, CT: Eno Foundation for Highway Traffic Control.

Reilly, W. R. (1984). Weaving analysis procedures for the new highway capacity manual. Federal Highway Administration, Offices of Research & Development, Traffic ….

Ritis. (2022). https://ritis.org/intro.

Roess, R., & Uliero, J. (2008). Analysis of freeway weaving sections. Final Report, NCHRP Project, 3–75.

Roess, R P, Ulerio, J. M., Prassas, E. S., Schoen, J., Vandehey, M., Reilly, W., & Kittelson, W. (2008). Analysis of Freeway Weaving Sections (Final Report for NCHRP Project 3-75). Transportation Research Institute, Polytechnic University, Brooklyn, NY.

Roess, Roger P, McShane, W. R., & Pignataro, L. J. (1980). Revision of NCHRP Methodology for Analysis of Weaving-Area Capacity. Transportation Research Record, 772, 58–65.

Rouphail, Nagui M., Karr, Karr F., Chase, R. T., & Ahmed, I. (2020). Predicting lane change intensity within urban interchange influence areas (IIA) (Report No. RP 2019-29).

Rouphail, N. M., Aghdashi, B., Elefteriadou, L., Amini, E., & Xu, D. (2021). Assessing and Addressing Deficiencies in the HCM Weaving Segment Analyses. Southeastern Transportation Research, Innovation, Development and Education ….

Schroeder, B. J. (2019). Update of Highway Capacity Manual : Merge, Diverge, and Weaving Methodologies. In National Cooperative Highway Research Program . NCHRP 07-26. https://apps.trb.org/cmsfeed/TRBNetProjectDisplay.asp?ProjectID=4553.

Skabardonis, Alex, & Kim, A. M. (2010). Weaving analysis, evaluation and refinement.

Skabardonis, Alexander, & Mauch, M. (2015). Evaluation of methodologies for analyzing freeway ramp weaving. Transportation Research Record, 2483(1), 130–139.

Skabardonis, Alexander, Papadimitriou, F., Halkias, B., & Kopelias, P. (2016). Operational Analyses of Freeway Off-Ramp Bottlenecks. Transportation Research Procedia, 15, 573–582.

Windover, J. R., & May, A. D. (1994). Revisions to level D methodology of analyzing freeway ramp weaving sections. Transportation Research Record, 1457.

Xu, D., Rouphail, N. M., Aghdashi, B., Ahmed, I., & Elefteriadou, L. (2020). Modeling framework for capacity analysis of freeway segments: application to ramp weaves. Transportation Research Record, 2674(1), 148–159.

Xu, Y., Williams, B. M., Rouphail, N. M., & Chase, R. T. (2013). Development of an Oversaturated Speed–Flow Model Based on the Highway Capacity Manual. Transportation Research Record, 2395(1), 41–48.

Zhou, C., Rong, J., Wang, S., & Feng, X. (2015). An Assessment Research on the predicted model of weaving speed in the 2010 HCM.